

Living Radical Polymerization of Acrylates Mediated by 1,3-Bis(2-pyridylimino)isoindolatocobalt(II) Complexes: Monitoring the Chain Growth at the Metal

Björn K. Langlotz,^[a] Julio Lloret Fillol,^[a] Jürgen H. Gross,^[b] Hubert Wadepohl,^[a] and Lutz H. Gade*^[a]

Abstract: A new type of mediator for cobalt(II)-mediated radical polymerization is reported which is based on 1,3-bis(2-pyridylimino)isoindolate (bpi) as ancillary ligand. The modular synthesis of the bis(pyridylimino)isoindoles (bpiH) employed in this work is based on the condensation of 2-aminopyridines with phthalodinitriles. Reaction of the bpiH protio-ligands with a twofold excess of cobalt(II) acetate or cobalt(II) acetylacetonate in methanol gave [Co(bpi)(OAc)], which crystallize as coordination polymers, and a series of [Co(acac)(bpi)(MeOH)], which are mononuclear octahedral complexes. Upon heating the [Co(acac)(bpi)(MeOH)] compounds to 100°C under high vacuum, the coordinated methanol was removed to give the five-coordinate complexes [Co(acac)(bpi)]. The

polymerization of methyl acrylate at 60°C was investigated by using one molar equivalent of the relatively short-lived radical source 2,2'-azobis(4-methoxy-2,4-dimethylvaleronitrile) (V-70) as initiator (monomer/catalyst/V-70: 600:1:1). The low solubility of the acetato complexes inhibits their significant activity as mediators in this reaction, whereas the acetylacetonate complexes control the radical polymerization of methyl acrylate more effectively. The radical polymerizations of the hexacoordinate complexes did not show a linear increase in number-average molecular weight (M_n) with conver-

sion; however, the polydispersities were relatively low (PDI=1.12–1.40). By using the pentacoordinate complexes [Co(acac)(bpi)] as mediators, a linear increase in M_n values with conversion, which were very close to the theoretical values for living systems, and very low polydispersities (PDI < 1.13) were obtained. This was also achieved in the block copolymerization of methyl acrylate and *n*-butyl acrylate. The intermediates with the growing acrylate polymer radical (PA) were identified by liquid injection field desorption/ionization mass spectrometry as following the general formula [Co(acac)(4-methoxy-bpi)-(MA)_{*n*}-R] (MA: methyl acrylate; R: C(CH₃)(CH₂C(CH₃)₂OCH₃)CN), a notion also confirmed by NMR end-group analysis.

Keywords: acrylates • cobalt • mass spectrometry • polymerization • radical reactions

Introduction

The control of radical polymerizations with the aim of suppressing chain terminations and chain transfer has been the focus of recent intense research. It has become a powerful method for the synthesis of a range of well-defined function-

alized homo- and copolymers.^[1] These processes are based on the activity of a regulator, a metal complex in most cases, which directly or indirectly controls the level of free-radical concentration.^[2]

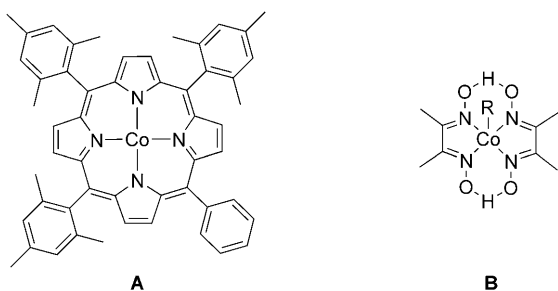
The most thoroughly studied mechanism, the atom-transfer radical polymerization (ATRP) introduced by Matyjaszewski and Sawamoto, involves metal complexes as radical mediators which reversibly transfer halogen atoms to radical chains.^[3–7] Alternatively, a reversible homolytic bond cleavage of a dormant polymer chain with a nitroxide^[8] or an organometallic complex (organometallic radical polymerization, OMRP)^[9–17] proved to be efficient. Finally, the thermodynamically quasi-neutral bimolecular exchange between propagating radical chains and a dormant species (degenerative transfer (DT) polymerization) may be operative.^[18–22]

[a] B. K. Langlotz, Dr. J. Lloret Fillol, Prof. Dr. H. Wadepohl, Prof. Dr. L. H. Gade
Anorganisch-Chemisches Institut, Universität Heidelberg
Im Neuenheimer Feld 270, 69120 Heidelberg (Germany)
Fax: (+49) 6221-545609
E-mail: lutz.gade@uni-hd.de

[b] Dr. J. H. Gross
Organisch-Chemisches Institut, Universität Heidelberg
Im Neuenheimer Feld 270, 69120 Heidelberg (Germany)

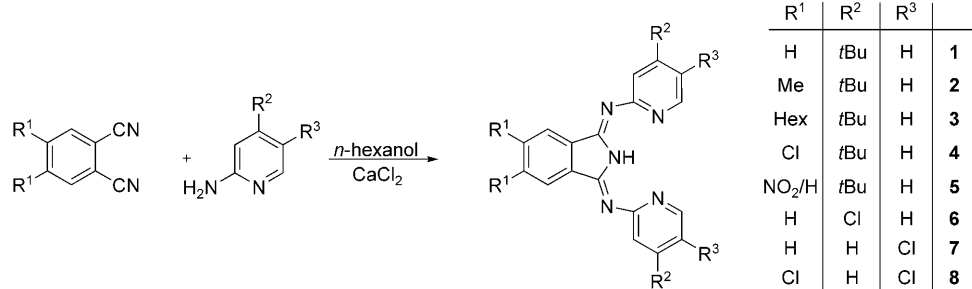
Organocobalt species, such as cobalt(II) tetramesitylporphyrin, have been shown to react in the polymerization of acrylates, acrylic acid and vinyl acetate by this DT mechanism if a slight excess of radicals is present during the reaction.^[23] The first example of cobalt-mediated radical polymerization (CMRP) was the polymerization of acrylates reported by Wayland et al. in the presence of cobalt porphyrin complexes, such as (tetramesitylporphyrin)cobalt (**A**).^[9,11] Later, alkylcobaloximes (**B**) were also found to be effective photoinitiators for the CMRP of acrylates.^[24] Other monomers, such as methacrylates, undergo hydrogen elimination; accordingly, for these monomers the mechanism involved catalytic chain-transfer polymerization (CCTP).^[25]

Herein, we report a new type of mediator for CMRP which is based on 1,3-bis(2-pyridylimino)isoindolates (bpi)^[26] as ancillary ligands for cobalt(II). The monoanionic meridionally coordinating bpi ligands are structurally related to phthalocyanines and porphyrins lacking the fourth coordinating N donor.^[27–35] As will be apparent below, pentacoordinate bpi–Co^{II} complexes act as efficient mediators for radical polymerizations of acrylates and give rise to living behavior. A principal objective of this work is the presentation of mechanistic insight into the processes during the initial period of the polymerization reaction, as well as the in situ detection of the intermediates of radical polymerization. This has been achieved for the first time by liquid injection field desorption/ionization (LIFDI) mass spectrometry.



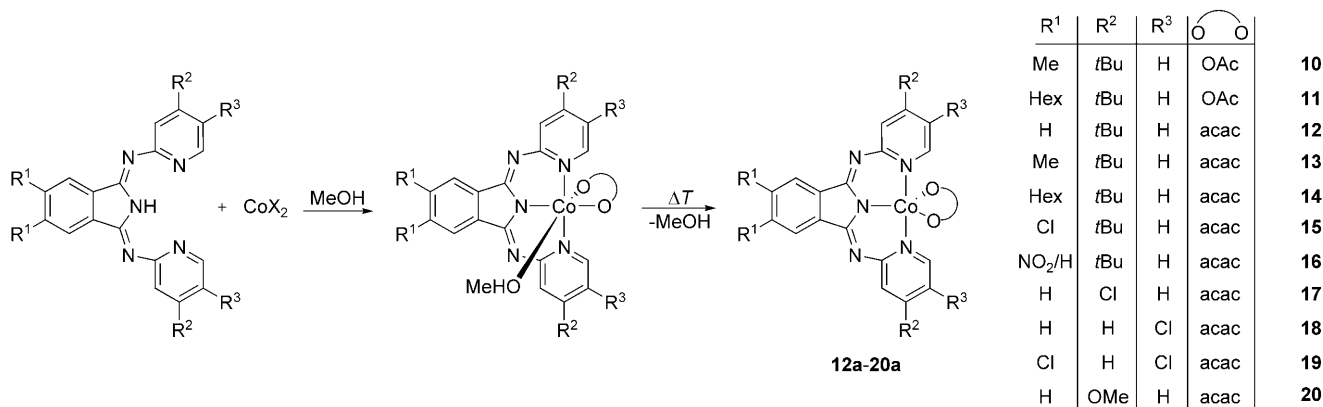
Results and Discussion

Synthesis and characterization of 1,3-bis(2-pyridylimino)isoindolates (bpi)–cobalt(II) complexes: The synthesis of the bpi ligands **1–9** employed in this work was based on a modification of the procedure originally published by Siegl.^[27,28,33,36] This modular synthesis from 2-aminopyridines and phthalodinitriles readily allows modifications in the *meta* and *para* positions of the pyridine rings as well as in the central isoindole unit (Scheme 1).



Scheme 1. Modular assembly of 1,3-bis(2-pyridylimino)isoindole protio-ligands by condensation of a substituted phthalonitrile and two molar equivalents of a 2-aminopyridine derivative.

Stirring the bpiH protio-ligands with a twofold excess of cobalt(II) acetate or cobalt(II) acetylacetonate in anhydrous methanol at room temperature gave the corresponding acetato (**10** and **11**) and acetylacetonato (**12–19** and **20a**) complexes as orange to dark-red microcrystalline solids in high yields (Scheme 2). Reducing the amount of cobalt(II) salt or increasing the reaction temperature led to the formation of the undesired symmetric octahedral



Scheme 2. Synthesis of a series of bpi–cobalt complexes.

[Co(bpi)₂] complexes. Both acetato complexes **10** and **11** are virtually insoluble in nonpolar solvents, such as benzene or toluene. In contrast, the acetylacetonato complexes display higher solubility in nonpolar as well as polar solvents.

For compounds **12–19**, the elemental analyses indicate the presence of one molecule of methanol per cobalt atom. It is thought to coordinate to the Co^{II} center, in the same way as established below for complex **19**, thus giving rise to octahedral coordination geometries with the general formula [Co(acac)(bpi)(MeOH)] (Scheme 2). In contrast, complex **20a**, containing the 4'-methoxy-bpi ligand, was directly isolated as a solvent-free compound. Upon heating all complexes to 100 °C under high vacuum, the coordinated methanol could be removed to give the methanol-free complexes **12a–19a** as indicated by their elemental analyses and a change of color to brown.

To establish the detailed molecular structures of the principal types of coordination compounds studied in this work, selected derivatives were examined by X-ray crystallography. Single crystals of the acetato complex **11** were grown from a saturated solution in methanol. As depicted in Figure 1, complex **11** aggregates as a coordination polymer in which each Co atom is coordinated by two bridging ace-

tate groups and one bpi ligand (Co(1)–O(1) 2.043(2), Co(2)–O(2) 2.022(2) Å). Such polymeric structures for the cobalt(II) acetate complexes seem to be responsible for the low solubility of the cobalt acetate complexes. The polymer chain adopts a meandering folded structure, as represented at the bottom of Figure 2.

Single crystals of complexes [Co(acac)(5'-chloro-bpi)] (**18a**), [Co(acac)(3,4-dichloro-5'-chloro-bpi)(MeOH)] (**19**), and [Co(acac)(3,4-dichloro-5'-chloro-bpi)] (**19a**) were obtained from hot toluene or benzene solutions. In contrast to the acetato complex **11**, the molecular structure of the acetylacetonato complex **19** is not polymeric. As already inferred from the analytical data, it contains one methanol molecule coordinated to the cobalt(II) center (Figure 2), which results in an octahedral coordination geometry. The Co–N(1) (2.021(2) Å) bond is significantly shorter than Co–N(3) (2.181(2) Å) and Co–N(5) (2.173(2) Å), which is due to the anionic character of N(1) and thus the amido-type coordination of this ligating atom.

In contrast to **19**, the molecular structures of the related complexes **18a** and **19a** are distorted trigonal bipyramidal with the isoindolato and the acac ligand occupying the equatorial and the two pyridyl groups the axial coordination sites

(Figure 3a and b). There are two very similar independent molecules in the asymmetric unit of **19a**. The Co–O distances of the acetylacetonato ligands in all the structures are in the expected range for cobalt(II)acetylacetonato complexes (**18a**: Co–O 2.009(1), 1.993(1) Å; **19**: Co–O 2.059(1), 2.045(1) Å; **19a**: Co–O 2.007(1)/1.990(1) Å, 2.000(1)/2.000(1) Å).^[37–40]

Paramagnetic ¹H NMR spectra were recorded for all complexes. Relatively sharp resonances were observed as a consequence of the rapid electron relaxation in the d⁷ systems. Based on the variation of the substitution pattern [stepwise exchange of the aromatic protons with chloro (compounds **17–19**), *tert*-butyl (compounds **12–16**) or methoxy groups (compound **20a**)], it was possible to assign all aromatic resonances for the complexes **12–20** (Table 1). The signals of the protons in the 6' position and the CH group of the acetylacetonato ligand are characteristically broadened and shifted downfield. The ¹H NMR signal

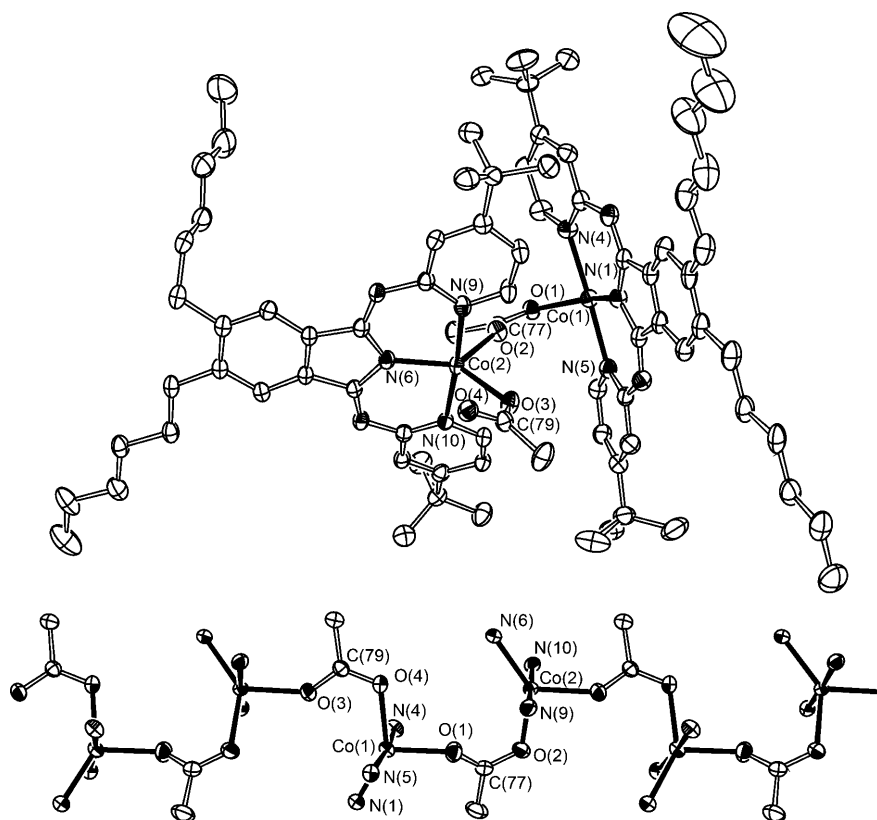


Figure 1. Molecular structure of complex **11**; hydrogen atoms are omitted for clarity. Top: asymmetric unit; bottom: polymeric chain. Selected bond lengths [Å] and angles [°]: Co(1)–N(1), 1.983(2), Co(1)–N(4) 2.131(2), Co(1)–N(5) 2.119(2), Co(1)–O(1) 2.043(2), Co(1)–O(4) 2.012(2), Co(2)–N(6) 1.975(2), Co(2)–N(9) 2.095(2), Co(2)–N(10) 2.159(2), Co(2)–O(2) 2.022(2), Co(2)–O(3) 2.005(2), C(77)–O(1) 1.258(3), C(77)–O(2) 1.264(3); N(1)–Co(1)–N(4) 86.62(7), N(1)–Co(1)–N(5) 88.81(7), N(4)–Co(1)–N(5) 173.60(7), N(1)–Co(1)–O(1) 146.03(7), N(1)–Co(1)–O(4) 117.68(8), O(1)–C(77)–O(2) 121.5(2), N(6)–Co(2)–N(9) 88.32(8), N(6)–Co(2)–N(10) 87.69(7), N(9)–Co(2)–N(10) 175.43(7), N(6)–Co(2)–O(2) 126.39(7), N(6)–Co(2)–O(3) 137.55(7).

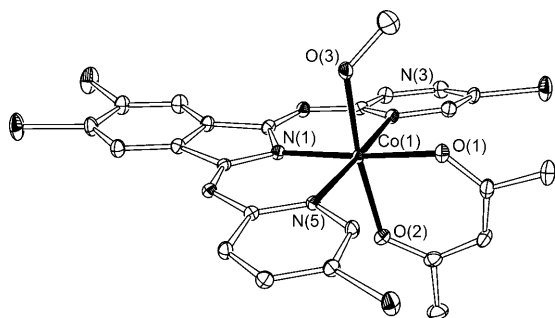


Figure 2. Molecular structure of complex **19**; hydrogen atoms are omitted for clarity. Selected bond lengths [Å] and angles [°]: Co–N(1) 2.021(2), Co–N(3) 2.181(2), Co–N(5) 2.173(2), Co–O(1) 2.059(1), Co–O(2) 2.0445(1); N(1)–Co–O(1) 174.70(6), N(5)–Co–N(3) 173.27(6), O(2)–Co–O(3) 170.35(5).

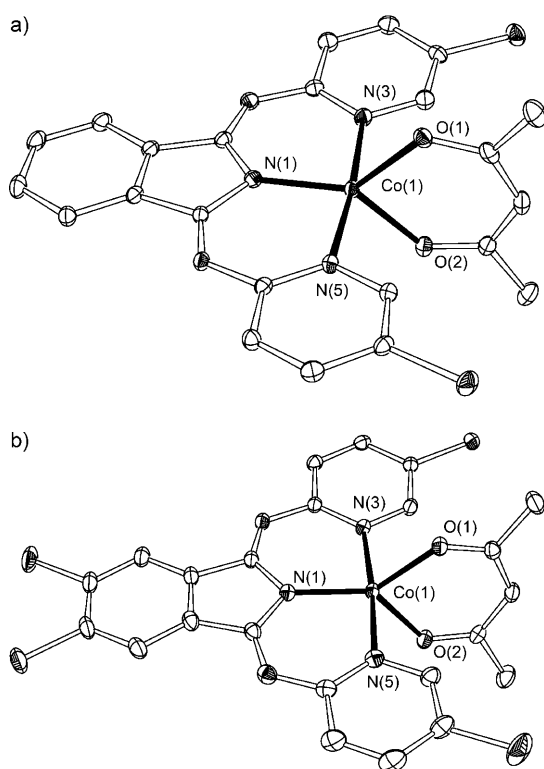


Figure 3. a) Molecular structure of complex **18a**; hydrogen atoms are omitted for clarity. Selected bond lengths [Å] and angles [°]: Co–N(1) 1.969(1), Co–N(3) 2.169(1), Co–N(5) 2.148(1), Co–O(1) 2.009(1), Co–O(2) 1.993(1); N(1)–Co–O(2) 136.34(5), N(1)–Co–O(1) 132.65(5), O(2)–Co–O(1) 90.98(4); b) Molecular structure of complex **19a**; only one of the two independent molecules is shown, and hydrogen atoms are omitted for clarity. Selected bond lengths [Å] and angles [°]; values given in square brackets refer to the second molecule: Co(1)–N(1) 1.9720(14) [1.9618(15)], Co(1)–N(3) 2.1537(15) [2.1458(16)], Co(1)–N(5) 2.1574(14) [2.1539(16)], Co(1)–O(1) 2.0070(12) [1.9903(13)], Co(1)–O(2) 1.9995(13) [2.0004(13)]; N(1)–Co(1)–O(2) 124.31(6) [137.06(6)], N(1)–Co(1)–O(1) 144.64(6) [131.10(6)], O(2)–Co(1)–O(1) 91.05(5) [91.74(5)].

of the CH_3 group of the coordinated methanol was broad and observed at $\delta = 0.5$ ppm, whereas the resonance of the OH proton could not be detected.

Variable-temperature ^1H NMR spectroscopic studies revealed the expected Curie–Weiss behavior for the paramagnetically shifted resonances of complexes **10–20** (Figure 4 for complex **20a**) in the temperature range of 233 to 373 K. Furthermore, the paramagnetic susceptibility of all complexes was measured by the Evans method.^[41] All magnetic moments are in good accordance with high-spin Co^{II} species ($\mu_{\text{M}} = 4.17\text{--}4.53 \mu_{\text{B}}$).

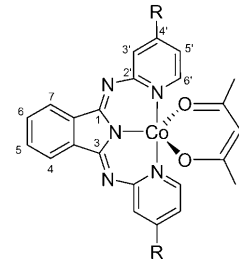
Polymerization of acrylates in the presence of [Co(acac)(bpi)(MeOH)] complexes with V-70: To assess the properties of complexes **10–20** as moderators in CMRP, we investigated the polymerization of methyl acrylate at 333 K (monomer/catalyst/V-70: 600:1:1).^[18–22] To initiate the polymerization, one molar equivalent of the relatively short-lived radical source 2,2'-azobis(4-methoxy-2,4-dimethyl valeronitrile) (V-70) was used ($t_{1/2}$ (333 K) = 11 min).^[11] This leads to the formation of a modest excess of organic radicals (1.06 equiv) under these reaction conditions. The transfer efficiency under the reaction conditions used was measured (by NMR spectroscopy) to be 53%.^[42] This is in good agreement with published values.^[11,42] The excess of radicals significantly increases the rate of polymerization without a noticeable increase of the polydispersity.

The low solubility of the acetato complexes **10** and **11** inhibits their activity as mediators in this reaction. This applies even more for **10** (polydispersity index, PDI, of the polymer ≈ 2.80) than for the slightly more soluble complex **11**, which shows moderate activity as mediator in the polymerization of methyl acrylate (PDI of the polymer ≈ 1.6). Both complexes were therefore not further investigated for this type of application.

In part due to their greater solubility, the acetylacetonato complexes **12–19** mediate the radical polymerization of methyl acrylate more effectively than the acetato complexes under the same conditions. The polymerization with complexes **18** and **19**, which bear chloro substituents in the *meta* position relative to the coordinating N atom of the pyridine rings, does not display a significant induction period.^[23] In contrast, polymerizations with complexes **12–17** are characterized by induction periods which are due to the time required to convert all of the [Co(acac)(bpi)-R] species.

Radical polymerizations mediated by complexes **12–19** did not show a linear increase in number-average molecular weight (M_n) with conversion (Figure 5 for complex **19**). Nevertheless, the polydispersities for complexes **12–19** were relatively low (PDI = 1.14, 1.13, 1.12, 1.14, 1.14, 1.15, <1.40, and <1.27 for **12–19**, respectively). The variable induction periods and the nonlinear increase of M_n with conversion were thought to be due to the occupation of the sixth coordination site in **12–19** by methanol. Its dissociation is the prerequisite for the formation of Co–R species (R: polymer chain) and thus the effective control of the OMRP.

This interpretation was confirmed by the polymerizations of methyl acrylate and *n*-butyl acrylate in the presence of the five-coordinate complexes [Co(acac)(bpi)] (**12a–20a**)

Table 1. Assignment of the paramagnetic ^1H NMR resonances [ppm] recorded at 295 K.


	4/7	5/6	3'	4'	5'	6'	$\text{CH}_{3(\text{acac})}$	$\text{CH}_{(\text{acac})}$
12	3.5	31.0	45.6	-13.1 ^[a]	20.9	145.6	35.8	129.5
13	3.2	21.2	46.6	-13.1 ^[a]	21.0	146.4	36.1	131.0
14	3.2	— ^[b]	47.1	-13.1 ^[a]	21.1	147.2	36.6	131.4
15	3.1	—	47.3	-12.9 ^[a]	21.1	143.4	35.4	128.4
16	3.7/ 3.1	—/ 30.3	41.3/ 41.0	-12.4 ^[a]	21.5/ 21.3	143.7	35.2	126.8
17	3.2	29.5	43.3	—	18.4	139.0	33.7	123.8
18	3.1	29.2	44.0	-13.2	—	146.8	32.3	122.3
19	3.1	—	44.2	-13.4	—	146.9	32.2	121.8
20a	3.6	30.8	45.3	-10.4 ^[c]	18.9	145.4	36.5	124.0

[a] Chemical shifts of the corresponding *tert*-butyl resonances.

[b] Chemical shifts of the hexyl resonances: $\delta=21.4$ (s, 4H; $\text{H}^{1'}$), 15.4 (s, 4H; $\text{H}^{2'}$), 10.7 (s, 4H; $\text{H}^{3'}$), 7.7 (s, 4H; $\text{H}^{4'}$), 6.0 (s, 4H; $\text{H}^{5'}$), 4.2 ppm (s, 4H; $\text{H}^{6'}$).

[c] Chemical shift of the corresponding methoxy resonance.

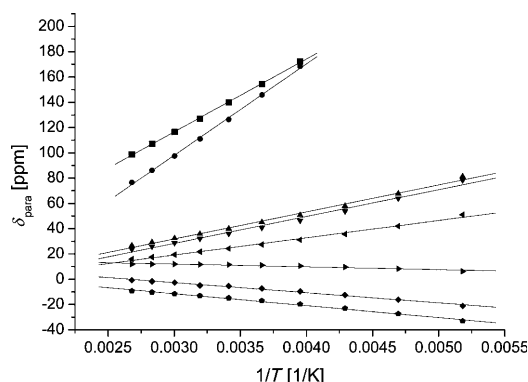
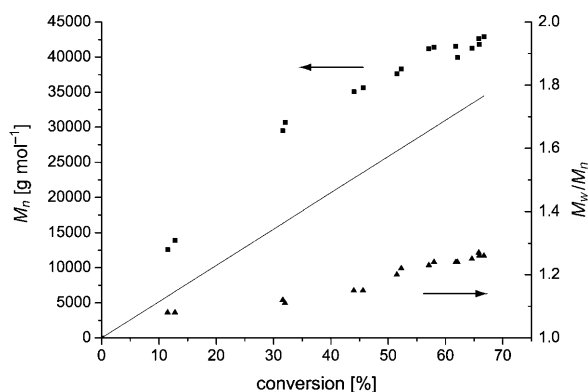
Figure 4. Curie plot of the ^1H NMR resonances of complex **20**.

Figure 5. Change in number-average molecular weight (M_n) and polydispersity with methyl acrylate conversion to poly(methyl acrylate) (PMA) for $[\text{Co}(\text{acac})(5,6\text{-dichloro-5-chloro-bpi})(\text{MeOH})]$ (**19**). (—): $M_n(\text{theor.})$, (■): $M_n(\text{measur.})$, (▲): PDI.

under the same conditions, which displayed a linear increase in M_n with conversion. Furthermore, the M_n values were found to be very close to the expected values for living systems and very low polydispersities ($\text{PDI} < 1.13$) were determined. This suggests that in these systems, close to one polymer chain per cobalt–bpi complex is growing with similar speed (Figure 6).

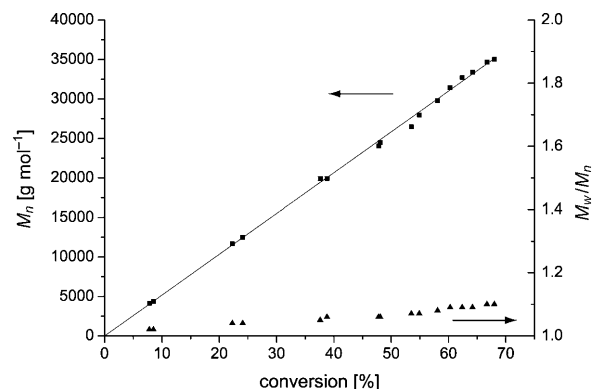


Figure 6. Change in number-average molecular weight (M_n) and polydispersity with methyl acrylate conversion to PMA for $[\text{Co}(\text{acac})(4\text{-methoxy-bpi})]$ (**20a**). (—): $M_n(\text{theor.})$, (■): $M_n(\text{measur.})$, (▲): PDI.

We further examined the capability of complex **20a** to act as a mediator in the block copolymerization of methyl acrylate and *n*-butyl acrylate. A low-polydispersity poly(methyl acrylate) block was generated initially as described above. Unreacted monomer was then removed under high vacuum, and the cobalt-end-capped polymers subsequently dissolved in a solution of *n*-butyl acrylate to restart the polymerization and generate the poly(methyl acrylate)–poly(butyl acrylate) block copolymer. A linear increase in the M_n with conversion of *n*-butyl acrylate and low polydispersity ($M_w/M_n < 1.15$; M_w : weight-average molecular weight) were also observed during this second stage of polymerization in the presence of complex **20a** and the formation of the block copolymer (Figure 7 and Table 2).

The polymerization of methyl acrylate with all methanol-free complexes (**12a–20a**) showed virtually superimposable results, which indicated no significant effect of the coordination pattern of the bpi ligands (Figure 8 for complexes **12a** and **19a**). This finding was unexpected because the application of bpi derivatives as ancillary ligands in a variety of catalysts had previously indicated a significant influence of the substitution pattern.

To investigate and analyse this result, a DFT study was carried out for the representative complexes **12a** and **18a–20a**.^[43,44] In general, good agreement with the computed minima and experimentally determined structural data was obtained by the B3LYP functional. Both high-spin ($S=3/2$) and low-spin ($S=1/2$) states were considered in our studies. In all cases the high-spin (hs) state was found to be more stable than the low-spin (ls) state, which is in agreement with the experimental data. (The zero-point vibrational en-

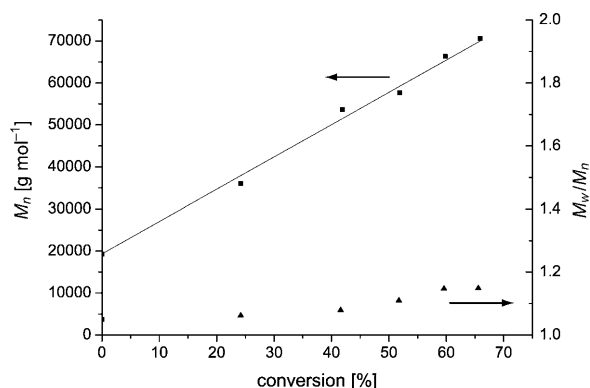


Figure 7. Change in number-average molecular weight (M_n) and polydispersity with *n*-butyl acrylate conversion to PMA–poly(butyl acrylate) block copolymer initiated by a [Co(acac)(4-methoxy-*bpi*)-PMA] block (derived from **20a**): conversion of initial methyl acrylate polymerization: 34.6%, $M_n = 19300 \text{ g mol}^{-1}$, $M_w/M_n = 1.05$. (—): $M_{n(\text{theor})}$, (■): $M_{n(\text{measured})}$, (▲): PDI.

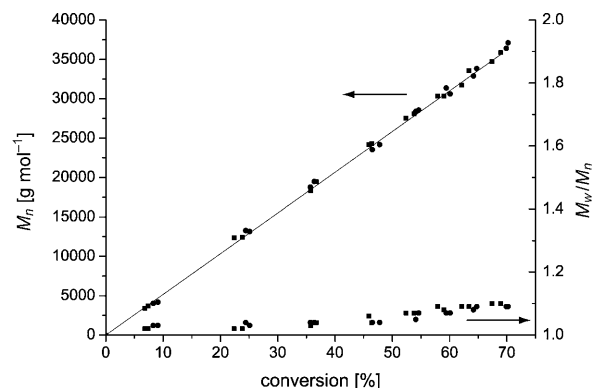


Figure 8. Change in number-average molecular weight (M_n) and polydispersity with methyl acrylate conversion to PMA for [Co(acac)(4-*t*Bu-*bpi*)] (**12a**) (■) and [Co(acac)(3,4-dichloro-5'-chloro-*bpi*)] (**19a**; ●). (—): $M_{n(\text{theor})}$ as well as the corresponding PDIs.

Table 2. Controlled radical polymerization of acrylates in the presence of [Co(acac)(*bpi*)]^[a]

Entry	Catalyst	Monomer	Z [%] ^[b]	$M_{n,\text{GPC}}$ [10^3 g mol^{-1}] ^[c]	$M_{n,\text{theor}}$ [10^3 g mol^{-1}] ^[d]	$M_{n,\text{theor}}$ [10^3 g mol^{-1}] ^[e]	M_w/M_n
1	10	MA	61.1	32.6	31.6	29.8	2.83
2	11	MA	63.0	32.5	32.5	30.7	1.64
3	12	MA	61.1	32.6	31.6	29.8	1.14
4	12a	MA	70.2	37.1	36.3	34.2	1.09
4	13	MA	63.1	34.3	32.6	30.8	1.12
5	14	MA	63.5	35.6	32.8	30.9	1.11
6	15	MA	65.6	35.0	33.9	32.0	1.14
7	16	MA	60.4	36.1	31.2	29.4	1.14
8	17	MA	63.2	32.7	32.6	30.8	1.15
9	18	MA	69.5	40.6	35.9	33.9	1.40
10	19	MA	66.7	42.9	34.5	32.5	1.27
11	19a	MA	68.9	35.9	35.6	33.6	1.10
12	20a	MA	68	35.0	35.1	33.1	1.10
13	20a	BA	65.9	56.3	50.7	47.8	1.13
14	20a	MA/BA ^[f]	65.9 ^[g]	70.6	70.0	66.1	1.15

[a] General conditions: 1 equiv [Co^{II}], 1 equiv V-70, 600 equiv monomer ($[M]_0/[Co^{II}]_0 = 600$) as 2N solution in benzene. [b] The monomer conversion Z is determined by integration of ¹H resonances of the monomer and the corresponding resonances of the polymer; values are averages of at least two runs. [c] Determined by gel-permeation chromatography (GPC) analyses with poly(*n*-butyl acrylate) calibration; values are averages of at least two runs. [d] $M_{n,\text{theor}}$ based on [Co^{II}]: $M_{n,\text{theor}} = ([M]_0/[Co^{II}]_0) \times M_{\text{monomer}} \times Z$. [e] $M_{n,\text{theor}}$ based on radical concentration: $M_{n,\text{theor}} = ([M]_0/[R]_0) \times M_{\text{monomer}} \times Z$. [f] General conditions: 1 equiv PMA appended to **20a** ($M_n = 19.3 \times 10^3 \text{ g mol}^{-1}$, $M_w/M_n = 1.05$), 600 equiv *n*-butyl acrylate (BA) as 2N solution in benzene. [g] Corresponds to the conversion of *n*-butyl acrylate; values are averages of at least two runs.

ergies $\Delta E_{\text{zp}}^{(s-t)}$ of [Co(acac)(3,4-dichloro-5'-chloro-*bpi*)] (**19a**), [Co(acac)(5-chloro-*bpi*)] (**18a**), [Co(acac)(*t*Bu-*bpi*)] (**12a**), and [Co(acac)(4'-methoxy-*bpi*)] (**20a**) were computed to be 6.1, 5.8, 4.6, and 4.5 kcal mol⁻¹, respectively.)

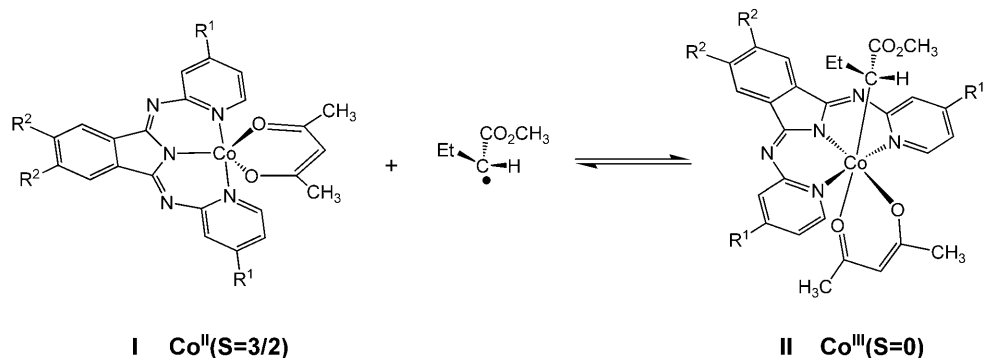
The cobalt(III)–R intermediates in the polymerization process of methyl acrylate were modelled by simulating the radical polymer chain as the α -methyl butyrate radical (R') [CH₃CH₂C(•)HCO₂Me]. The introduction of this additional coordinative fragment to the metal center gave rise to octahedral [Co^{III}] low-spin complexes in all cases (Scheme 3).

The stabilization due to the formation of the Co–R bond in [Co^{III}–R] low-spin complexes from the Co^{II} high-spin complexes and the free radical (R•) is represented by the

bond dissociation energy (BDE) of the Co–R bond. The computed energies represented in Table 3 confirm the ability of 1,3-bis(pyridylimino)isoindolato–Co^{II} complexes to stabilize radicals, but these values are much smaller than literature data for experimental Co–C BDEs.^[45] It has been demonstrated recently that the nonhybrid functional BP86^[46] is able to reproduce the Co–C BDEs of organocobalt complexes in a more accurate manner.^[47] We therefore also computed the BDEs by using the BP86 functional. The results summarized in Table 3 show that the BP86 BDE energies are in the expected range.^[45] In agreement with the experimental results, the variation of the BDEs for the selected complexes **12a** and **18a–20a** is only very small (<2 kcal mol⁻¹). These results

show clearly that there is no significant electronic influence of the substitution pattern of the ligand on the BDE.

In addition, both the lengths of the carbon–cobalt bond ($d(\text{C}–\text{Co}) = (2.055 \pm 0.001) \text{ \AA}$) and the natural bond orbital charges on the cobalt ($q(\text{Co}) = (0.984 \pm 0.001) e$) are not influenced by the different substitution patterns of the ligands. Closer inspection of the frontier orbitals of the Co–*bpi* complexes reveals that the sigma skeleton of the ligand is orthogonal to the Co–C bond, thus explaining the observed and calculated minor influence of the substitution pattern on the Co–C bond reactivity. Furthermore, the molecular orbital analysis also clearly indicates the negligible interaction of the ligand π system with the Co–C bond (Figure 9).

Scheme 3. Equilibrium between Co^{II} -bpi high-spin complexes with a free radical and the Co^{III} -bpi low-spin complex bearing the radical.Table 3. Formation energy of intermediates $\text{II}_{\text{a-d}}$ from $\text{I}_{\text{a-d}}$ in Scheme 3.^[a]

Isomer	R^1	R^2	B3LYP		BP86	
			BDE	ΔG	BDE	ΔG
a	Cl	Cl	-4.9	13.1	-28.0	-10.0
b	Cl	H	-5.2	13.1	-28.1	-10.3
c	<i>t</i> Bu	H	-6.4	12.0	-29.2	-10.9
d	MeO	H	-6.3	11.7	-30.0	-11.5

[a] $\Delta E = E[\text{I}_{\text{a-d}}] + E[\text{R}] - E[\text{II}_{\text{a-d}}]$; R : α -methyl butyrate radical [$\text{CH}_3\text{CH}_2\text{C}(\cdot)\text{HCO}_2\text{Me}$].

In summary, the Co–C bond appears to be electronically decoupled from the substituents on the bpi systems. These may be thus appropriately chosen to control other molecular properties of the Co^{II} mediators in the polymerization, such as the solubility in a particular reaction medium.

Identification of reactive intermediates by mass spectrometry and NMR end-group analysis: As already discussed above, it is generally believed that the formation of an organometallic complex [$\text{Co}^{\text{III}}\text{-R}$] is the key step during the induction period of the CMRP of acrylates. Scheme 4 summarizes the dominant reactions that are thought to occur within this initial period.^[23,11]

Homolytic dissociation of the radical source V-70 generates a tertiary carbon-centered radical ([Eq. (1)] in Scheme 4) followed by the abstraction of an H atom by a Co^{II} species to form a cobalt hydrido species [Eq. (2)]. This transient species reacts with one molecule of acrylate monomer to form an alkyl complex [Eq. (3)], which in turn undergoes thermal homolytic cleavage of the Co–C bond to produce an organic radical ([Eq. (4)] in Scheme 4). The latter initiates alkyl acrylate polymerization to form an oligomer radical ([Eq. (5)] in Scheme 4) that binds again to the Co^{II} species ([Eq. (6)] in Scheme 4). Due to the persistent radical effect the growth of the polymeric radical has living character in the last stage of the induction period. After this period the mechanism gradually changes to a DT process,^[23] which is indicated by the setting in of rapid polymerization.

To obtain insight into the processes involved during the induction period of CMRP, that is, prior to the DT stage, the composition of the reaction mixture was monitored by

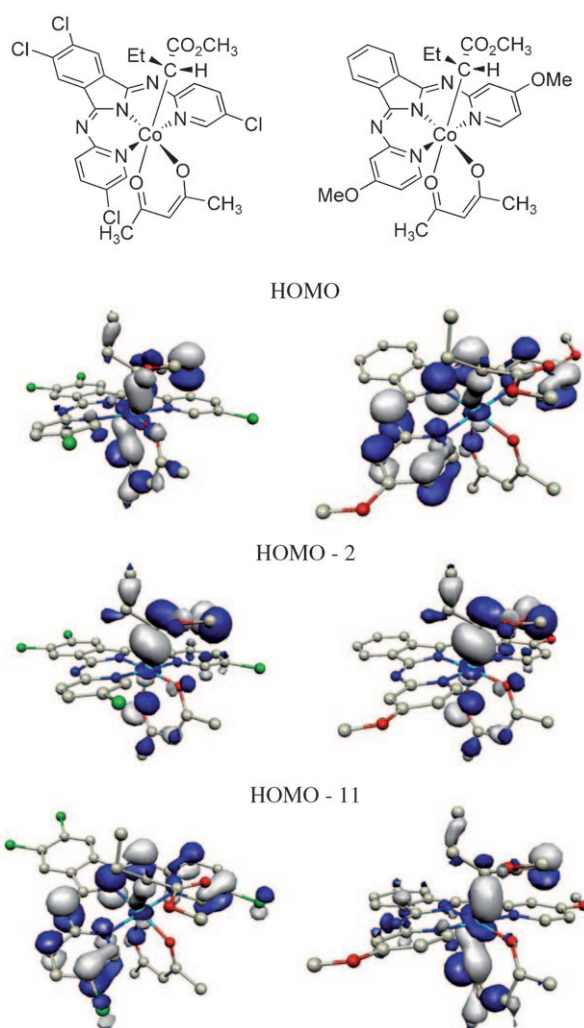
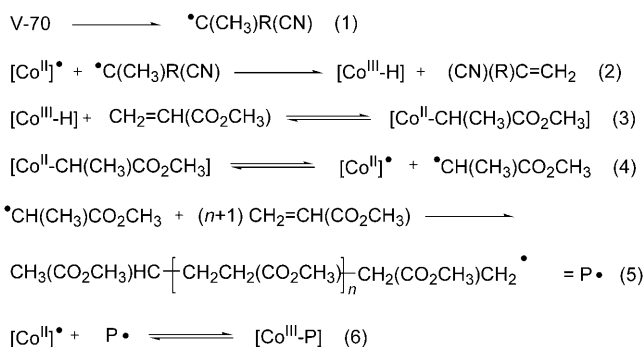


Figure 9. Representation of the key occupied molecular frontier orbitals involved in the Co–C bond for the organocobalt complexes derived from **19a** (left) and **20a** (right). The almost complete decoupling of ligand-centered molecular orbitals is clearly visible.

mass spectrometry. LIFDI was chosen, because it combines the soft ionization of field desorption (FD)^[48] with the inertness required to analyse extremely moisture- and air-sensitive compounds.^[49]



Scheme 4. Proposed scheme of dominant reactions during the induction time of the CMRP of acrylates.^[11,23]

The LIFDI spectrum of the polymerization of methyl acrylate (MA) is dominated by a peak at m/z 516.1 that can be assigned to complex **20a**. This ion is detected in high abundance during the induction period and represents a major fragment of $[\text{Co}(\text{acac})(4\text{-methoxy-bpi})\text{-}(\text{MA})_n\text{-H}]$. The additional peak at m/z 1032.2 corresponds to a $[\text{Co}(\text{acac})(4\text{-methoxy-bpi})]_2^{2+}$ cluster ion, such species being frequently detected in FD-mass spectrometry.^[50] Setting the rather narrow m/z 900–1300 range allowed sufficient resolution to be maintained at a comparatively fast scan rate. This turned out to be important to detect the intermediates during their short period of desorption.

During the first 10 min of the polymerization several organometallic species consisting of $[\text{Co}(\text{acac})(4\text{-methoxy-bpi})]$ and oligomer chains of variable chain length could be reproducibly detected. We were able to observe organometallic species containing methyl acrylate units and an end group derived from the dissociation of the radical source V-70 following the general formula $[\text{Co}(\text{acac})(4\text{-methoxy-bpi})\text{-}(\text{MA})_n\text{-R}]$ with $\text{R}=\text{C}(\text{CH}_3)(\text{CH}_2\text{C}(\text{CH}_3)_2\text{OCH}_3)\text{CN}$. This is in contrast to the proposed formation of a cobalt hydrido species ([Eq. (2)] in Scheme 4), which subsequently forms organometallic species that consist only of methyl acrylate units ([Eq. (3)] and the following in Scheme 4). The observed organometallic species contained between three and seven methyl acrylate units (Figure 10).

The fragmentation of mass-selected ions upon collision-induced dissociation (CID) was employed to confirm the presumed composition of the observed species.^[51] The tandem mass spectra were obtained by admitting helium collision gas into the collision chamber of the first field-free region and analysing the fragments by scanning the instrument at constant B/E .^[52] In each case the tandem mass spectrometry experiment showed the presence of the $[\text{Co}(\text{acac})(4\text{-methoxy-bpi})]$ fragments at m/z 516 and 417, which may be assigned to $[\text{Co}(4\text{-methoxy-bpi})]^+$ (Figure 11).

To further substantiate these results, we performed end-group analyses of the polymers by ^1H NMR experiments. As marker signal of the end group $-\text{C}(\text{CH}_3)(\text{CH}_2\text{C}(\text{CH}_3)_2\text{OCH}_3)\text{CN}$ we chose the methoxy group, because its resonance is well separated from the signals of the polymer chain. In each case we were able to identify the end group

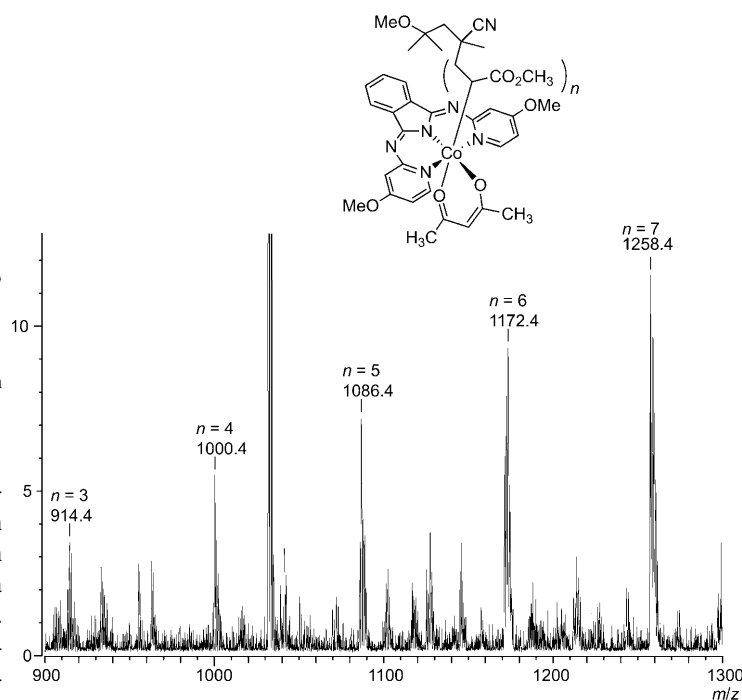


Figure 10. LIFDI mass spectrum obtained during the polymerization of methyl acrylate with complex **20** and V-70 as radical source after 7 min (intensity scale expanded by a factor of 8 to better show the relevant signals). Organometallic species of the type $[\text{Co}(\text{acac})(4\text{-methoxy-bpi})\text{-}(\text{MA})_n\text{-R}]$ with $n=3\text{--}7$ were detected, that is, $n=3$ at m/z 914.4 (calcd: 914.3), $n=4$ at m/z 1000.4 (calcd: 1000.4), $n=5$ at m/z 1086.4 (calcd: 1086.4), $n=6$ at m/z 1172.4 (calcd: 1172.4) and $n=7$ at m/z 1258.4 (calcd: 1258.5).

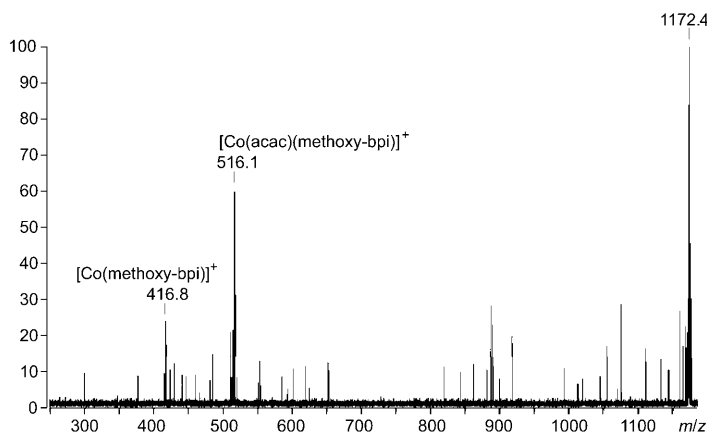


Figure 11. Representative CID mass spectrum of a polymerizing complex. Here, the mass spectrum of the precursor ion at m/z 1172.4, which corresponds to $[\text{Co}(\text{acac})(4\text{-methoxy-bpi})\text{-}(\text{MA})_6\text{-R}]^+$ with $\text{R}=\text{C}(\text{CH}_3)(\text{CH}_2\text{C}(\text{CH}_3)_2\text{OCH}_3)\text{CN}$, is shown.

by a resonance at $\delta=3.15$ ppm, and its integral ratio with the methoxy group of the polymer ($\delta=3.65$ ppm) was in very good agreement with the integral ratio calculated from the molecular weight obtained by GPC. We therefore assume that cobalt-bpi complexes are not able to undergo a fast $\beta\text{-H}$ abstraction from the starter radical as proposed by

Wayland et al. for their cobalt porphyrin complexes.^[11,23] Instead, we propose an initial reaction sequence as represented in Scheme 5.



Scheme 5. Modified scheme of the initial reactions in the [Co(bpi)]-controlled radical polymerization of methyl acrylate (without the previously proposed β -hydride abstraction step).

Conclusions

A new class of radical mediators based on bpi-Co^{II} complexes, which effectively control the living radical polymerization of acrylates, has been established. The facile one-step synthesis of the ancillary bpi ligands and the following complexation step render the new complexes suitable for broader applications in this field.

These systems proved to be particularly suited to the direct monitoring of the chain growth at the metal center in a first LIFDI mass spectrometric study of such a process. Whilst the previously proposed general mechanistic schemes for OMRP are vindicated to a large extent, it is notable that in the case at hand there is no indication of β -H abstraction from the starter radical. An investigation into what degree this also applies to other OMRP systems is under way.

Experimental Section

General: All manipulations were carried out by standard Schlenk line or glovebox techniques under an atmosphere of argon. Solvents were pre-dried over activated 4 Å molecular sieves and were refluxed over potassium (benzene, benzene-*d*₆), magnesium (methanol) or calcium hydride (methyl acrylate, butyl acrylate) under an argon atmosphere and collected by distillation. CDCl₃ was dried over calcium hydride, distilled under reduced pressure and stored under argon in Teflon-valve ampoules. ¹H and ¹³C{¹H} NMR spectra were recorded on Bruker Avance III 600, Bruker Avance II 400 and Bruker DRX 200 spectrometers. ¹H and ¹³C NMR assignments were confirmed when necessary by the use of distortionless enhancement by polarization transfer with a 135° decoupler pulse (DEPT-135) and two-dimensional ¹H-¹H and ¹³C-¹H NMR experiments. ¹H and ¹³C NMR spectra were referenced internally to residual protio-solvent (¹H) or solvent (¹³C) resonances and are reported relative to tetramethylsilane ($\delta=0$ ppm). GPC analyses were carried out on a PSS MCS2031 Compact System equipped with three PSS SDV columns working with THF as mobile phase at a flow rate of 1.00 mL min⁻¹ at 23 °C. All measurements are relative to poly(*n*-butyl acrylate) standards from PSS (Polymer Standards Service, Mainz, Germany). Samples for infrared spectroscopy were prepared as KBr pellets and spectra were recorded on a Varian Excalibur 3100 series FTIR spectrometer. Infrared data are quoted in wave numbers (cm⁻¹). Elemental analyses were performed by the analytical services of the University of Heidelberg. Measurements of the magnetic susceptibility were carried out according to the method developed by Evans.^[41] 2-Amino-4-*tert*-butylpyridine^[53] and 2-amino-4-methoxypyridine^[54] were prepared according published methods. All other compounds and reagents were obtained from commercial suppliers and used without further purification. V-70 was handled at -78 °C.

Preparation of the compounds

General procedure for the preparation of the 1,3-bis(2-pyridylimino)isoindoles (given for 6): A suspension of phthalonitrile (0.72 g, 5.54 mmol), 2-amino-4-chloropyridine (1.64 g, 12.74 mmol) and CaCl₂ (0.28 g, 2.78 mmol) in 1-hexanol (20 mL) was heated at reflux for 18 h. After the mixture had been cooled to room temperature, the yellow precipitate was isolated by filtration, washed with hexane to remove 1-hexanol (20 mL), dissolved in dichloromethane (20 mL), and the solution was filtered through celite and dried in vacuo to provide **6** (1.71 g, 4.65 mmol; 84% yield). Compounds **1–9** were synthesized accordingly.

5,6-Dimethyl-4-*t*-Bu-bpi (2): Yield: 71%; m.p.: 220 °C; ¹H NMR (399.90 MHz, CDCl₃, 295 K): $\delta=13.90$ (s, 1H; NH), 8.49 (d, 2H, ³J_{H,H}=5.3 Hz; H⁶), 7.87 (s, 2H; H⁴⁺), 7.47 (d, ⁴J_{H,H}=1.8 Hz, 2H; H³), 7.11 (dd, 2H, ³J_{H,H}=5.3, ⁴J_{H,H}=1.8 Hz; H⁵), 2.43 (s, 6H; CH₃), 1.36 ppm (s, 18H; C(CH₃)₃); ¹³C{¹H} NMR (100.57 MHz, CDCl₃, 293 K): $\delta=162.3$ (s, C²), 160.5 (s, C⁴), 154.1 (s, C¹⁺³), 147.5 (s, C⁶), 141.1 (s, C⁵⁺⁶), 133.5 (s, C⁸⁺⁹), 123.3 (s, C⁴⁺), 119.8 (s, C³), 117.5 (s, C⁵), 34.8 (s, C(CH₃)₃), 30.5 (s, C(CH₃)₃), 20.4 ppm (s, CH₃); IR (KBr): $\tilde{\nu}=3251$ (br), 2979 (m), 2934 (m), 1634 (s), 1588 (vs), 1474 (s), 1352 (w), 1231 (w), 1110 (w) cm⁻¹; MS (EI+): *m/z* (%): 439.3 [M]⁺; elemental analysis calcd (%) for C₂₈H₃₃N₅+CH₂Cl₂ (439.60): C 71.01, H 7.11, N 14.53; found: C 70.77, H 7.16, N 14.43.}}}}

5,6-Dihexyl-4-*t*-Bu-bpi (3): Yield: 72%; m.p.: 202 °C; ¹H NMR (399.90 MHz, CDCl₃, 295 K): $\delta=13.89$ (s, 1H; NH), 8.50 (d, 2H, ³J_{H,H}=5.3 Hz; H⁶), 7.85 (s, 2H; H⁴⁺), 7.45 (d, 2H, ⁴J_{H,H}=1.8 Hz; H³), 7.10 (dd, 2H, ³J_{H,H}=5.3, ⁴J_{H,H}=1.8 Hz; H⁵), 2.75 (t, 4H, ³J_{H,H}=3.6 Hz; H^{1'}), 1.68 (m, 4H; H^{2'-5'}), 1.36 (m, 12H; H^{2'-5'}), 1.36 (s, 18H; C(CH₃)₃), 0.91 ppm (t, 6H, ³J_{H,H}=7.1 Hz; CH₃); ¹³C{¹H} NMR (100.57 MHz, CDCl₃, 295 K): $\delta=162.3$ (s, C²), 160.8 (s, C⁴), 154.2 (s, C¹⁺³), 147.6 (s, C⁶), 145.3 (s, C⁵⁺⁶), 133.5 (s, C⁸⁺⁹), 122.9 (s, C⁴⁺), 119.9 (s, C³), 117.5 (s, C⁵), 34.9 (s, C(CH₃)₃), 33.4 (s, C^{1'}), 31.8 (s, C^{2'}), 31.2 (s, C^{3'}), 30.6 (s, C(CH₃)₃), 29.6 (s, C^{4'}), 22.6 (s, C^{5'}), 14.1 ppm (s, C^{6'}); IR (KBr): $\tilde{\nu}=3243$ (br), 2998 (m), 2929 (m), 1630 (s), 1587 (vs), 1472 (s), 1351 (w), 1220 (w), 1109 (w) cm⁻¹; MS (EI+): *m/z* (%): 579.4 [M]⁺; elemental analysis calcd (%) for C₃₈H₅₃N₅ (579.86): C 78.71, H 9.21, N 12.08; found: C 78.72, H 9.06, N 12.11.}}}}}}

5,6-Dichloro-4-*t*-Bu-bpi (4): Yield: 79%; m.p.: 203 °C; ¹H NMR (600.13 MHz, CDCl₃, 295 K): $\delta=14.04$ (s, 1H; NH), 8.53 (d, 2H, ³J_{H,H}=5.3 Hz; H⁶), 8.17 (s, 2H; H⁴⁺), 7.47 (d, 2H, ⁴J_{H,H}=1.4 Hz; H³), 7.17 (dd, 2H, ³J_{H,H}=5.3, ⁴J_{H,H}=1.4 Hz; H⁵), 1.39 ppm (s, 18H; *t*Bu); ¹³C{¹H} NMR (150.90 MHz, CDCl₃, 295 K): $\delta=162.6$ (s, C²), 160.1 (s, C⁴), 151.6 (s, C¹⁺³), 147.7 (s, C⁶), 136.0 (s, C⁸⁺⁹), 135.2 (s, C⁵⁺⁶), 124.4 (s, C⁴⁺), 120.4 (s, C³), 118.1 (s, C⁵), 34.9 (s, C(CH₃)₃), 30.6 ppm (s, C(CH₃)₃); IR (KBr): $\tilde{\nu}=3221$ (m, br), 2967 (m), 2877 (w), 1628 (m), 1584 (s), 1547 (m), 1488 (s), 1401 (w), 1360 (w), 1283 (m), 1262 (w), 1222 (w), 1202 (w), 1027 (w), 921 (m), 830 (m) cm⁻¹; MS (EI+): *m/z* (%): 479.2 (100) [M]⁺, 464.1 (17.0) [M-CH₃]⁺; elemental analysis calcd (%) for C₂₆H₂₇Cl₂N₅ (479.43): C 65.00, H 5.66, N 14.58; found: C 64.72, H 5.72, N 14.38.}}}}

5-Nitro-4-*t*-Bu-bpi (5): Yield: 74%; m.p.: 198 °C; ¹H NMR (399.90 MHz, CDCl₃, 295 K): $\delta=14.18$ (s, 1H; NH), 8.88 (s, 1H, ⁴J=1.8 Hz; H⁴), 8.53 (d, 1H, ³J_{H,H}=5.4 Hz; H⁶), 8.52 (d, 1H, ³J_{H,H}=5.2 Hz; H⁶), 8.47 (dd, 1H, ³J_{H,H}=8.2, ⁴J_{H,H}=1.79 Hz; H⁵), 8.19 (d, 1H, ³J_{H,H}=8.2 Hz; H⁷), 7.50 (d, 1H, ⁴J_{H,H}=1.6 Hz; H³), 7.49 (d, 1H, ⁴J_{H,H}=1.5 Hz; H³), 7.17 (dd, 1H, ³J_{H,H}=5.4, ⁴J_{H,H}=1.6 Hz; H⁵), 7.16 (dd, 2H, ³J_{H,H}=5.2, ⁴J_{H,H}=1.5 Hz; H⁷), 1.38 (s, 9H; C(CH₃)₃), 1.37 ppm (s, 9H; C(CH₃)₃); ¹³C{¹H} NMR (100.57 MHz, CDCl₃, 295 K): $\delta=162.7$ (s, C²), 162.6 (s, C²), 159.9 (s, C^{4+4'}), 151.4 (s, C³), 151.2 (s, C¹), 150.3 (s, C⁵), 147.8 (s, C⁶), 147.7 (s, C^{6'}), 141.3 (s, C⁹), 137.2 (s, C⁸), 126.4 (s, C⁶), 123.4 (s, C⁷), 120.7 (s, H³), 120.6 (s, H^{3'}), 118.4 (s, C⁵), 118.3 (s, H^{5'}), 118.1 (s, C⁴), 34.9 (s, C(CH₃)₃), 30.5 ppm (s, C(CH₃)₃); IR (KBr): $\tilde{\nu}=3247$ (m, br), 2968 (m), 2936 (w), 2845 (w), 1621 (m), 1588 (s), 1531 (m), 1457 (m), 1362 (w), 1328 (m), 1264 (m), 1100 (m), 902 (m), 819 (m) cm⁻¹; MS (EI+): *m/z* (%): 456.2 (100) [M]⁺, 441.1 (31.4) [M-CH₃]⁺, 399.2 (14.1) [M-C₄H₉]⁺, 322.1 (25.3) [M-*tert*-butylpyridyl]⁺; elemental analysis calcd (%) for 2C₂₆H₂₈N₆O₂ (456.54)+methanol: C 67.35, H 6.40, N 17.78; found: C 67.57, H 6.11, N 17.99.}}}}}}}}}}}

4'-Chloro-bpi (6): Yield: 84%; m.p.: 202 °C; ¹H NMR (600.13 MHz, CDCl₃, 295 K): $\delta=13.76$ (s, 1H; NH), 8.47 (d, 2H, ³J_{H,H}=5.4 Hz; H⁶),}

8.05 (m, 2H; H⁵⁺⁶), 7.68 (m, 2H; H⁴⁺⁷), 7.49 (d, 2H, ⁴J_{H,H}=1.7 Hz; H³), 7.14 ppm (dd, 2H, ³J_{H,H}=5.4, ⁴J_{H,H}=1.7 Hz; H⁵); ¹³C{¹H} NMR (150.90 MHz, CDCl₃, 293 K): δ=161.4 (C²), 154.4 (C¹⁺³), 148.3 (C⁶), 145.3 (C⁴), 135.5 (C⁸⁺⁹), 132.0 (C⁵⁺⁶), 123.4 (C³), 122.8 (C⁴⁺⁷), 120.5 ppm (C⁵); IR (KBr): $\tilde{\nu}$ =3225 (br), 2970 (m), 2923 (m), 1630 (s), 1590 (vs), 1476 (s), 1356 (w), 1235 (w), 1112 (w) cm⁻¹; HRMS (EI+): *m/z* 367.0398, calcd for C₁₈H₁₁Cl₂N₅: 367.0392; elemental analysis calcd (%) for C₁₈H₁₁Cl₂N₅ (367.04): C 58.71, H 3.01, N 19.02; found: C 58.63, H 3.08, N 18.91.

5,6-Dichloro-5'-chloro-bpi (8): Yield: 92%; m.p.: 206 °C; ¹H NMR (600.13 MHz, CDCl₃, 295 K): δ=13.68 (s, 1H; NH), 8.61 (d, 2H, ⁴J_{H,H}=2.7 Hz; H⁶), 8.15 (s, 2H; H⁴⁺⁷), 7.80 (dd, 2H, ³J_{H,H}=8.5, ⁴J_{H,H}=2.7 Hz; H⁴), 7.43 ppm (d, 2H, ³J_{H,H}=8.5 Hz; H³); ¹³C{¹H} NMR (150.90 MHz, CDCl₃, 293 K): δ=158.6 (C²), 151.9 (C¹⁺³), 147.0 (C⁶), 138.5 (C⁴), 136.6 (C⁵⁺⁶), 135.5 (C⁸⁺⁹), 124.9 (C³), 128.8 (C⁵), 124.8 ppm (C⁴⁺⁷); IR (KBr): $\tilde{\nu}$ =3234 (br), 2993 (m), 2943 (m), 1627 (s), 1589 (vs), 1478 (s), 1351 (w), 1239 (w), 1109 (w) cm⁻¹; HRMS (EI+): *m/z* 434.9605, calcd for C₁₈H₉Cl₄N₅: 434.9612; elemental analysis calcd (%) for C₁₈H₉Cl₄N₅ (434.96): C 49.46, H 2.08, N 16.02; found: C 49.32, H 2.11, N 15.86.

4'-Methoxy-bpi (9): Yield: 80%; m.p.: 198 °C; ¹H NMR (600.13 MHz, CDCl₃, 295 K): δ=14.06 (s, 1H; NH), 8.45 (d, 2H, ³J_{H,H}=5.6 Hz; H⁶), 8.11 (m, 2H; H⁵⁺⁶), 7.69 (m, 2H; H⁴⁺⁷), 7.03 (d, 2H, ⁴J_{H,H}=2.3 Hz; H³), 6.74 (dd, 2H, ³J_{H,H}=5.5, ⁴J_{H,H}=2.3 Hz; H⁵), 3.96 ppm (s, 6H; OCH₃); ¹³C{¹H} NMR (150.90 MHz, CDCl₃, 293 K): δ=167.3 (C⁴), 162.3 (C²), 153.9 (C¹⁺³), 148.5 (C⁶), 135.8 (C⁸⁺⁹), 131.6 (C⁴⁺⁷), 122.5 (C⁵⁺⁶), 108.3 (C⁵), 107.1 (C³), 55.3 ppm (OCH₃); IR (KBr): $\tilde{\nu}$ =3222 (br), 2978 (m), 2923 (m), 1632 (s), 1592 (vs), 1483 (s), 1347 (w), 1236 (w), 1135 (w) cm⁻¹; HRMS (EI+): *m/z* 359.1365, calcd for C₂₀H₁₇N₅O₂: 359.1382; elemental analysis calcd (%) for C₂₀H₁₇N₅O₂ (359.38): C 66.84, H 4.77, N 19.49; found: C 66.67, H 4.79, N 19.18.

General procedure for the synthesis of complexes 10–20: The respective ligand (1.00 mmol) was added at once to a stirred suspension of cobalt acetylacetonate (514 mg, 2.00 mmol; for complexes **10** and **11** cobalt acetate was used) in dry methanol (10 mL). After 16 h the precipitate was isolated by filtration, washed three times with small quantities of methanol and dried in a vacuum.

General procedure for removing coordinated methanol: The corresponding cobalt acetylacetonate complex was heated at 100 °C in high vacuum for 48 h. During that time the color change gradually from orange (**12**) or red (**19**) to brown.

[Co(diMe-*t*Bu-bpi)(OAc) (10): Yield: 79 %, m.p.: 147 °C; ¹H NMR (199.92 MHz, [D₆]DMSO, 295 K): δ=98.6 (s, 2H), 74.0 (s, 2H), 24.9 (s, 2H), 19.9 (s, 2H), 12.4 (s, 6H; CH₃), 2.0 (s, 3H; OAc), -10.0 ppm (s, 18H; *t*Bu); IR (KBr): $\tilde{\nu}$ =2999 (m), 2938 (m), 1633 (s), 1628 (s), 1595 (vs), 1483 (s), 1344 (w), 1221 (w), 1108 (w) cm⁻¹; μ_B =4.28 B; HRMS (FAB+): *m/z* 497.1956 ([M-OAc]⁺), calcd for C₂₈H₃₂CoN₅: 497.1990; elemental analysis calcd (%) for C₃₀H₃₅CoN₅O₂·MeOH (556.56): C 63.26, H 6.68, N 11.90; found: C 62.83, H 6.67, N 11.75.

[Co(dihexyl-*t*Bu-bpi)(OAc) (11): Yield: 81 %, m.p.: 143 °C; ¹H NMR (199.92 MHz, [D₆]DMSO, 295 K): δ=99.3 (s, 2H), 74.2 (s, 2H), 25.0 (s, 2H), 20.0 (s, 2H), 12.2 (s, 4H; CH₃), 7.8 (s, 4H), 5.7 (s, 4H), 4.3 (s, 4H), 3.6 (s, 4H), 2.0 (s, 3H; OAc), 1.4 (s, 6H), -10.0 ppm (s, 18H; *t*Bu); IR (KBr): $\tilde{\nu}$ =2997 (m), 2935 (s), 2916 (m), 1635 (s), 1634 (s), 1587 (s), 1481 (s), 1348 (w), 1209 (w), 1111 (w) cm⁻¹; μ_B =4.25 B; HRMS (FAB+): *m/z* 637.3528 (M-OAc)⁺, calcd for C₃₈H₅₂CoN₅: 637.3555; elemental analysis calcd (%) for C₄₀H₅₅CoN₅O₂·H₂O (696.83): C 67.21, H 8.04, N 9.80; found: C 67.44, H 7.73, N 10.01.

[Co(acac)(*t*Bu-bpi)(MeOH) (12): Yield: 82 %, m.p.: 128 °C; ¹H NMR (199.92 MHz, C₆D₆, 295 K): δ=145.6 (s, 2H; H⁵), 129.5 (s, 1H; H⁷), 45.6 (s, 2H; H²), 35.8 (s, 6H; H³), 31.0 (s, 2H; H²), 20.9 (s, 2H; H⁴), 3.5 (s, 2H; H²), 0.5 (s, 3H; CH₃OH), -13.1 ppm (s, 18H; *t*Bu); IR (KBr): $\tilde{\nu}$ =2990 (m), 2926 (m), 1638 (s), 1621 (s), 1589 (vs), 1487 (s), 1352 (w), 1234 (w), 1116 (w) cm⁻¹; μ_B =4.33 B; HRMS (ESI+): *m/z* 569.2196, calcd for C₃₁H₃₆CoN₅O₂: 569.2201; elemental analysis calcd (%) for C₃₁H₃₅CoN₅O₂·MeOH (632.66): C 62.65, H 6.75, N 11.07; found: C 62.93, H 6.50, N 11.24.

[Co(acac)(*t*Bu-bpi) (12a): Elemental analysis calcd (%) for C₃₁H₃₅CoN₅O₂ (568.58): C 65.49, H 6.20, N 12.32; found: C 65.78, H 6.31, N 12.19.

[Co(acac)(5,6-dimethyl-4-*t*Bu-bpi)(MeOH) (13): Yield: 81 %, m.p.: 132 °C; ¹H NMR (199.92 MHz, C₆D₆, 295 K): δ=146.4 (s, 2H; H⁶), 131.0 (s, 1H; CH), 46.6 (s, 2H; H³), 36.1 (s, 6H; CH₃(acac)), 21.2 (s, 6H; CH₃), 21.0 (s, 2H; H⁵), 3.2 (s, 2H; H⁴⁺⁷), 0.5 (s, 3H; CH₃OH), -13.1 ppm (s, 18H; C(CH₃)₃); IR (KBr): $\tilde{\nu}$ =2997 (m), 2934 (m), 1633 (s), 1624 (s), 1587 (vs), 1481 (s), 1343 (w), 1224 (w), 1110 (w) cm⁻¹; μ_B =4.27 B; HRMS (ESI+): *m/z* 597.2528 [M+H]⁺, calcd for C₃₃H₄₀CoN₅O₂: 597.2514; elemental analysis calcd (%) for C₃₃H₃₉N₅CoO₂·MeOH (628.67): C 64.96, H 6.89, N 11.14; found: C 64.72, H 6.69, N 11.23.

[Co(acac)(5,6-dimethyl-4-*t*Bu-bpi) (13a): Elemental analysis calcd (%) for C₃₃H₃₉N₅CoO₂ (596.63): C 66.43, H 6.59, N 11.74; found: C 66.29, H 6.62, N 11.51.

[Co(acac)(5,6-dihexyl-4-*t*Bu-bpi)(MeOH) (14): Yield: 76 %, m.p.: 122 °C; ¹H NMR (199.92 MHz, C₆D₆, 295 K): δ=147.2 (s, 2H; H⁶), 131.4 (s, 1H; CH), 47.1 (s, 2H; H³), 36.6 (s, 6H; CH₃(acac)), 21.4 (s, 4H; H¹), 21.1 (s, 2H; H⁵), 15.4 (s, 4H; H²), 10.7 (s, 4H; H³), 7.7 (s, 4H; H⁴), 6.0 (s, 4H; H⁵), 4.2 (s, 6H; H⁶), 3.2 (s, 2H; H⁴⁺⁷), 0.4 (s, 3H; CH₃OH), -13.1 ppm (s, 18H; C(CH₃)₃); IR (KBr): $\tilde{\nu}$ =2956 (m), 2930 (m), 1629 (s), 1616 (s), 1589 (vs), 1487 (s), 1310 (w), 1235 (w), 1084 (w) cm⁻¹; μ_B =4.32 B; HRMS (ESI+): *m/z* 737.4099 [M+H]⁺, calcd for C₄₅H₆₀CoN₅O₂: 737.4079; elemental analysis calcd (%) for C₄₃H₅₉N₅CoO₂·2MeOH (800.97): C 67.48, H 8.43, N 8.74; found: C 67.10, H 8.29, N 8.77.

[Co(acac)(5,6-dihexyl-4-*t*Bu-bpi) (14a): Elemental analysis calcd (%) for C₄₃H₅₉N₅CoO₂ (736.89): C 70.09, H 8.07, N 9.50; found: C 70.21, H 7.98, N 9.37.

[Co(acac)(5,6-dichloro-4-*t*Bu-bpi)(MeOH) (15): Yield: 84 %, m.p.: 137 °C; ¹H NMR (199.92 MHz, C₆D₆, 295 K): δ=143.4 (s, 2H; H⁶), 128.4 (s, 1H; CH), 47.3 (s, 2H; H³), 35.4 (s, 6H; CH₃(acac)), 21.1 (s, 2H; H⁵), 3.1 (s, 2H; H⁴⁺⁷), 0.5 (s, 3H; CH₃OH), -12.9 ppm (s, 18H; C(CH₃)₃); IR (KBr): $\tilde{\nu}$ =2996 (m), 2918 (m), 1639 (s), 1622 (s), 1572 (vs), 1492 (s), 1323 (w), 1210 (w), 1009 (w) cm⁻¹; μ_B =4.30 B; HRMS (ESI+): *m/z* 636.1340 [M+H]⁺, calcd for C₃₁H₃₄CoN₅O₂Cl₂: 636.1343; elemental analysis calcd (%) for C₃₁H₃₃N₅CoO₂·MeOH (669.51): C 57.41, H 5.57, N 10.46; found: C 57.05, H 5.55, N 10.42.

[Co(acac)(5,6-dichloro-4-*t*Bu-bpi) (15a): Elemental analysis calcd (%) for C₃₁H₃₃N₅CoO₂ (637.47): C 57.41, H 5.22, N 10.99; found: C 57.21, H 5.35, N 10.74.

[Co(acac)(5-nitro-4-*t*Bu-bpi)(MeOH) (16): Yield: 86 %, m.p.: 131 °C; ¹H NMR (199.92 MHz, C₆D₆, 295 K): δ=143.7 (s, 2H; H⁶), 126.8 (s, 1H; CH), 41.3 (s, 1H; H³), 41.0 (s, 1H; H²), 35.2 (s, 6H; CH₃(acac)), 30.3 (s, 1H; H⁵), 21.5 (s, 1H; H⁵), 21.3 (s, 1H; H⁵), 3.7 (s, 1H; H⁴⁺⁷), 3.1 (s, 1H; H⁴⁺⁷), 0.4 (s, 3H; CH₃OH), -12.4 ppm (s, 18H; C(CH₃)₃); IR (KBr): $\tilde{\nu}$ =2996 (m), 2933 (m), 1632 (s), 1621 (s), 1587 (vs), 1474 (s), 1347 (w), 1228(w), 1111 (w) cm⁻¹; μ_B =4.23 B; HRMS (ESI+): *m/z* 614.2045 [M+H]⁺, calcd for C₃₁H₃₅CoN₅O₆: 614.2052; elemental analysis calcd (%) for C₃₁H₃₄N₅CoO₂·MeOH (613.57): C 59.53, H 5.93, N 13.02; found: C 59.41, H 5.82, N 13.19.

[Co(acac)(5-nitro-4-*t*Bu-bpi) (16a): Elemental analysis calcd (%) for C₃₁H₃₄N₅CoO₂ (613.57): C 60.68, H 5.59, N 13.70; found: C 60.59, H 5.71, N 13.52.

[Co(acac)(4-chloro-bpi)(MeOH) (17): Yield: 85 %, m.p.: 136 °C; ¹H NMR (199.92 MHz, C₆D₆, 295 K): δ=139.0 (s, 2H; H⁵), 123.8 (s, 1H; H⁷), 43.3 (s, 2H; H²), 33.7 (s, 6H; H⁶), 29.5 (s, 2H; H³), 18.4 (s, 2H; H⁴), 3.2 (s, 2H; H²), 0.5 ppm (s, 3H; CH₃OH); IR (KBr): $\tilde{\nu}$ =2992 (m), 2921 (m), 1642 (s), 1628 (s), 1578 (vs), 1486 (s), 1341 (w), 1221 (w), 1106 (w) cm⁻¹; μ_B =4.22 B; HRMS (FAB+): *m/z* 524.0072, calcd for C₂₃H₁₇Cl₂CoN₅O₂: 524.0091; elemental analysis calcd (%) for C₂₃H₁₇Cl₂CoN₅O₂·MeOH (557.29): C 51.72, H 3.80, N 12.57; found: C 51.44, H 3.78, N 12.39.

[Co(acac)(4-chloro-bpi) (17a): Elemental analysis calcd (%) for C₂₃H₁₇Cl₂CoN₅O₂ (525.25): C 52.59, H 3.26, N 13.33; found: C 52.51, H 3.49, N 13.01.

[Co(acac)(5'-chloro-bpi)(MeOH) (18): Yield: 80 %, m.p.: 143 °C; ¹H NMR (199.92 MHz, C₆D₆, 295 K): δ=146.8 (s, 2H; H⁵), 122.3 (s, 1H;

H⁷), 44.0 (s, 2H; H²), 32.3 (s, 6H; H⁶), 29.2 (s, 2H; H³), 3.1 (s, 2H; H²), 0.4 (s, 3H; CH₃OH), -13.2 ppm (s, 2H; H³); IR (KBr): $\tilde{\nu}$ = 3003 (m), 2931 (m), 1636 (s), 1611 (s), 1585 (vs), 1473 (s), 1314 (w), 1218 (w), 1111 (w) cm⁻¹; μ_B = 4.17 B; HRMS (ESI+): m/z 525.0164, calcd for C₂₃H₁₈Cl₂CoN₅O₂: 525.0170; elemental analysis calcd (%) for C₂₃H₁₇Cl₂CoN₅O₂·MeOH (557.29): C 51.72, H 3.80, N 12.57; found: C 51.36, H 3.80, N 12.32.

[Co(acac)(5'-chloro-bpi)] (18a): Elemental analysis calcd (%) for C₂₃H₁₇Cl₂CoN₅O₂ (525.25): C 52.59, H 3.26, N 13.33; found: C 52.31, H 3.09, N 13.47.

[Co(acac)(3,4-dichloro-5'-chloro-bpi)(MeOH)] (19): Yield: 89%, m.p.: 139°C; ¹H NMR (199.92 MHz, C₆D₆, 295 K): δ = 146.9 (s, 2H; H²), 121.8 (s, 1H; H⁷), 44.2 (s, 2H; H²), 32.2 (s, 6H; H⁶), 3.1 (s, 2H; H²), 0.4 (s, 3H; CH₃OH), -13.4 ppm (s, 2H; H³); IR (KBr): $\tilde{\nu}$ = 2999 (m), 2927 (m), 1649 (s), 1602 (s), 1576 (vs), 1479 (s), 1328 (w), 1232 (w), 1098 (w) cm⁻¹; μ_B = 4.27 B; HRMS (ESI+): m/z 591.9306, calcd for C₂₃H₁₅Cl₄CoN₅O₂: 591.9312; elemental analysis calcd (%) for C₂₃H₁₅Cl₄CoN₅O₂·MeOH (626.18): C 46.09, H 3.06, N 11.18; found: C 45.81, H 3.12, N 11.07.

[Co(acac)(3,4-dichloro-5'-chloro-bpi)] (19a): Elemental analysis calcd (%) for C₂₃H₁₅Cl₄CoN₅O₂ (594.14): C 46.49, H 2.54, N 11.79; found: C 46.83, H 2.48, N 11.88.

[Co(acac)(4'-methoxy-bpi)] (20a): Yield: 79%, m.p.: 129°C; ¹H NMR (199.92 MHz, C₆D₆, 295 K): δ = 145.4 (s, 2H; H²), 124.0 (s, 1H; H⁷), 45.3 (s, 2H; H²), 36.5 (s, 6H; H⁶), 30.8 (s, 2H; H³), 18.9 (s, 2H; H⁴), 3.6 (s, 2H; H²), -10.4 ppm (s, 2H; OMe); IR (KBr): $\tilde{\nu}$ = 2996 (m), 2914 (m), 1632 (s), 1609 (s), 1591 (vs), 1486 (s), 1316 (w), 1224 (w), 1107 (w) cm⁻¹; μ_B = 4.31 B; HRMS (ESI+): m/z 517.1155, calcd for C₂₅H₂₄CoN₅O₄: 517.1160; elemental analysis calcd (%) for C₂₅H₂₄CoN₅O₄ (516.41): C 58.14, H 4.49, N 13.56; found: C 57.96, H 4.56, N 13.53.

Polymerizations

Acrylate polymerizations: In a typical polymerization a solution of alkyl acrylate (2M) in dry benzene (18 mmol, 9 mL) was added to a cobalt-bpi complex (0.03 mmol) and V-70 (0.03 mmol) in a Schlenk tube. This solution was immediately warmed to 60°C and stirred until the reaction was

completed. At given times the conversion was monitored by ¹H NMR spectroscopy and samples of 1 mL were taken. The polymer samples were precipitated with methanol and analysed by GPC.

Block copolymerization of butyl acrylate and methyl acrylate: A sample of poly(methyl acrylate) appended to [Co(acac)(4-methoxy-bpi)] (20a) was prepared as described. The solvent and unreacted monomer were removed by vacuum and a solution of butyl acrylate (2N) in benzene (18 mmol) was added. The Schlenk tube was heated to 60°C and at given times the conversion was monitored by ¹H NMR spectroscopy and samples of 1 mL were taken. The polymer samples were precipitated with methanol and analysed by GPC.

Online mass spectrometric experiments of acrylate polymerizations: LIFDI mass spectra and LIFDI tandem mass spectra were recorded on a JEOL JMS-700 magnetic sector mass spectrometer (JEOL, Tokyo, Japan) with FD ion source and a LIFDI probe (Linden CMS, Lesste, Germany). The instrument was set to a resolving power of 1300 and scanned at cycle times of about 5 s. Samples were taken at short time intervals during the induction period of the polymerization of methyl acrylate with complex 20a and V-70 as radical source. The samples were diluted 1:10 (v/v) in dry toluene under argon and immediately subjected to LIFDI mass spectrometry according to published procedures.^[55]

Positive-ion ESI mass spectra were obtained on a Bruker ApexQe Fourier transform ion cyclotron resonance (FT-ICR) mass spectrometer (Bruker Daltonik, Bremen, Germany). External mass calibration delivered mass accuracies in the order of 1 ppm. Typically, 16 transients of 1 m were accumulated for each mass spectrum.

X-ray crystal structure analyses: Crystal data and details of the structure determinations are listed in Table 4. Intensity data were collected at low temperature with a STOE IPDS 1 (11) and a Bruker AXS Smart 1000 CCD diffractometer (18a, 19 and 19a; MoK α radiation, graphite monochromator, λ = 0.71073 Å). Data were corrected for Lorentz and polarization effects;^[56] absorption was treated with a semiempirical multiscan method.^[57,58] The structures were solved by the heavy-atom method combined with structure expansion by direct methods applied to difference

Table 4. Details of the crystal structure determinations of the complexes 11, 18a, 19 and 19a.

	11	18a	19	19a
formula	C ₄₀ H ₅₅ CoN ₅ O ₂ · \approx 1.5 CH ₃ OH	C ₂₃ H ₁₇ Cl ₂ CoN ₅ O ₂ ·0.5 C ₆ H ₆	C ₂₄ H ₁₉ Cl ₄ CoN ₅ O ₃	C ₂₃ H ₁₅ Cl ₄ CoN ₅ O ₂ ·0.5 C ₇ H ₈
crystal system	monoclinic	triclinic	triclinic	monoclinic
space group	<i>P</i> 2/ <i>c</i>	<i>P</i> $\bar{1}$	<i>P</i> $\bar{1}$	<i>C</i> 2/ <i>c</i>
<i>a</i> [Å]	29.760(5)	7.7122(3)	8.1482(5)	37.849(5)
<i>b</i> [Å]	16.294(3)	11.3882(5)	12.3869(7)	13.670(2)
<i>c</i> [Å]	17.340(2)	13.8751(6)	12.8312(7)	26.895(4)
α [°]		91.991(1)	83.290(1)	
β [°]	91.420(15)	99.324(1)	89.196(1)	134.404(2)
γ [°]		94.092(1)	79.545(1)	
<i>V</i> [Å ³]	8406(2)	1198.13(9)	1264.81(13)	9942(2)
<i>Z</i>	8	2	2	16
<i>M_r</i>	744.88	564.30	626.17	617.16
ρ_{calcd} [Mg × m ⁻³]	1.177	1.564	1.644	1.649
<i>F</i> ₀₀₀	3200	576	634	4984
μ (MoK α) [mm ⁻¹]	0.451	0.975	1.139	1.156
max., min. transmission factors	0.9496, 0.8499	0.7464, 0.6916	0.7463, 0.6704	0.7464, 0.6677
data collect. temp. [K]	150(2)	100(2)	100(2)	100(2)
θ range [°]	1.7–24.1	1.8–32.2	1.7–30.5	1.5–32.3
index ranges (indep. set)	-34 ≤ <i>h</i> ≤ 34, 0 ≤ <i>k</i> ≤ 18, 0 ≤ <i>l</i> ≤ 19	-11 ≤ <i>h</i> ≤ 11, -16 ≤ <i>k</i> ≤ 16, 0 ≤ <i>l</i> ≤ 20	-11 ≤ <i>h</i> ≤ 11, -17 ≤ <i>k</i> ≤ 17, 0 ≤ <i>l</i> ≤ 18	-56 ≤ <i>h</i> ≤ 40, 0 ≤ <i>k</i> ≤ 20, 0 ≤ <i>l</i> ≤ 40
reflms measured	54016	30028	30519	251778
unique [<i>R</i> _{int}]	13187 [0.0606]	7861 [0.0458]	7699 [0.0487]	16894 [0.0374]
observed [<i>I</i> ≥ 2σ(<i>I</i>)]	8889	6221	5935	14348
parameters refined	903	327	340	672
<i>R</i> indices [<i>F</i> > 4σ(<i>F</i>)] <i>R</i> (<i>F</i>), <i>wR</i> (<i>F</i> ²)	0.0376, 0.0826	0.0361, 0.0880	0.0386, 0.0963	0.0399, 0.0951
<i>R</i> indices (all data) <i>R</i> (<i>F</i>), <i>wR</i> (<i>F</i> ²)	0.0605, 0.0873	0.0503, 0.0948	0.0561, 0.1018	0.0513, 0.1026
goodness-of-fit on <i>F</i> ²	0.871	1.072	1.222	1.076
largest residual peaks [e Å ⁻³]	0.379, -0.318	0.584, -0.350	1.414, -0.819	1.878, -1.294

structure factors (**11**),^[59] by direct methods with dual-space recycling (“shake-and-bake”, **18a**)^[60] or by conventional direct methods^[61,62] (**19** and **19a**) and refined by full-matrix least-squares methods based on F^2 .^[62,63] All non-hydrogen atoms were given anisotropic displacement parameters. All hydrogen atoms were placed in calculated positions and refined with a riding model.

Rather diffuse electron density, attributed to heavily disordered solvent, was found to occupy the channels between the polymeric chains in the structure of **11**. This density, approximately 150 electrons (ca. 8.4 molecules of methanol) per unit cell, was removed from the structure (and the corresponding F_{obs}) with the BYPASS/SQUEEZE procedure,^[64] as implemented in PLATON.^[65]

CCDC-693091 (**11a**), CCDC-693092 (**18a**), CCDC-680377 (**19**), and CCDC-693093 (**19a**) contain the supplementary crystallographic data for this paper. These data can be obtained free of charge from The Cambridge Crystallographic Data Centre via www.ccdc.cam.ac.uk/data_request/cif.

Computational studies: All the calculations were made with the Gaussian 03 program package.^[66] DFT^[43] calculations were performed with the unrestricted non-local hybrid B3LYP^[44] and the non-hybrid BP86^[46] functionals and a LANL2DZ basis set for the Co and 6-31G(d) basis sets for the other atoms.^[67] The molecular systems studied were optimized starting from X-ray diffraction data. Following geometry optimization, frequency calculations were performed on all calculated structures to ensure that there were no imaginary frequencies. All geometry optimizations were carried out without symmetry constraints. The $\langle S^2 \rangle$ values were found to be very close to the expected data, which indicated only minor spin contaminations. All energies were corrected for zero-point vibrational energies. BDEs and ΔG energies were obtained at 298 K.

Acknowledgement

This work was supported by the Deutsche Forschungsgemeinschaft (SFB 623). We also acknowledge the award of a doctoral scholarship by the Studienstiftung des Deutschen Volkes (to B.K.L.) and the EU (Marie Curie EIF fellowship to J.L.F.).

- [1] K. Matyjaszewski, T. P. Davis, *Handbook of Radical Polymerization*, Wiley-Interscience, New York, **2002**.
- [2] A. Goto, T. Fukuda, *Prog. Polym. Sci.* **2004**, *29*, 329.
- [3] J.-A. Wang, K. Matyjaszewski, *J. Am. Chem. Soc.* **1995**, *117*, 5614.
- [4] J.-S. Wang, K. Matyjaszewski, *Macromolecules* **1995**, *28*, 7901.
- [5] T. E. Patten, J. Xia, T. Abernathy, K. Matyjaszewski, *Science* **1996**, *272*, 866.
- [6] K. Matyjaszewski, J. Xia, *Chem. Rev.* **2001**, *101*, 2921.
- [7] M. Kamigaito, T. Ando, M. Sawamoto, *Chem. Rev.* **2001**, *101*, 3689.
- [8] C. J. Hawker, A. W. Bosman, E. Harth, *Chem. Rev.* **2001**, *101*, 3661.
- [9] B. B. Wayland, G. Poszmik, S. L. Mukerjee, M. Fryd, *J. Am. Chem. Soc.* **1994**, *116*, 7943.
- [10] B. B. Wayland, L. Basickes, S. L. Mukerjee, M. Wei, M. Fryd, *Macromolecules* **1997**, *30*, 8109.
- [11] Z. Lu, M. Fryd, B. B. Wayland, *Macromolecules* **2004**, *37*, 2686.
- [12] A. Debuigne, J.-R. Caille, R. Jerome, *Angew. Chem.* **2005**, *117*, 1125; *Angew. Chem. Int. Ed.* **2005**, *44*, 1101.
- [13] A. Debuigne, J.-R. Caille, C. Detrembleur, R. Jerome, *Angew. Chem.* **2005**, *117*, 3505; *Angew. Chem. Int. Ed.* **2005**, *44*, 3439.
- [14] A. Debuigne, J.-R. Caille, R. Jerome, *Macromolecules* **2005**, *38*, 5452.
- [15] A. Debuigne, J.-R. Caille, N. Willet, R. Jerome, *Macromolecules* **2005**, *38*, 9488.
- [16] R. Poli, *Angew. Chem.* **2006**, *118*, 5180; *Angew. Chem. Int. Ed.* **2006**, *45*, 5058.
- [17] M. Sebastien, H. Kaneyoshi, K. Matyjaszewski, R. Poli, *Chem. Eur. J.* **2007**, *13*, 2480.
- [18] S. G. Gaynor, J.-S. Wang, K. Matyjaszewski, *Macromolecules* **1995**, *28*, 8051.
- [19] M. C. Iovu, K. Matyjaszewski, *Macromolecules* **2003**, *36*, 9346.
- [20] S. Yamago, *J. Polym. Sci. Part A* **2006**, *44*, 1.
- [21] a) G. Moad, E. Rizzardo, S. H. Thang, *Polymer* **2008**, *49*, 1079; b) J. Chiefari, E. Rizzardo *Handbook of Radical Polymerization* (Eds.: K. Matyjaszewski, T. P. Davis), Wiley-Interscience, New York, **2002**, p. 629.
- [22] P. Corpart, D. Charmont, T. Biadatti, S. Z. Zard, D. Michelet, in *PCT Int. Appl.*, WO9858974, Rhodia, France, **1998**.
- [23] B. B. Wayland, C.-H. Peng, X. Fu, Z. Lu, M. Fryd, *Macromolecules* **2006**, *39*, 8219.
- [24] L. D. Arvanitopoulos, M. P. Greuel, H. J. Harwood, *Polym. Prepr.* **1994**, *35*, 549.
- [25] A. A. Gridnev, S. D. Ittel, *Chem. Rev.* **2001**, *101*, 3611.
- [26] J. A. Elvidge, R. P. Linstead, *J. Chem. Soc.* **1952**, 5000.
- [27] W. O. Siegl, *J. Org. Chem.* **1977**, *42*, 1872.
- [28] W. O. Siegl, *Inorg. Nucl. Chem. Lett.* **1974**, *10*, 825.
- [29] R. R. Gagné, W. A. Marritt, D. N. Marks, W. O. Siegl, *Inorg. Chem.* **1981**, *20*, 3260.
- [30] L. Saussine, E. Brazi, A. Robine, H. Mimoun, J. Fischer, R. Weiss, *J. Am. Chem. Soc.* **1985**, *107*, 3534.
- [31] E. T. Farinas, C. V. Nguyen, P. K. Mascharak, *Inorg. Chim. Acta* **1997**, *263*, 17.
- [32] F. A. Chavez, P. K. Mascharak, *Acc. Chem. Res.* **2000**, *33*, 539.
- [33] M. B. Meder, L. H. Gade, *Eur. J. Inorg. Chem.* **2004**, 2716.
- [34] M. B. Meder, B. A. Siggelkow, L. H. Gade, *Z. Anorg. Allg. Chem.* **2004**, *630*, 1962.
- [35] B. K. Langlotz, H. Wadepohl, L. H. Gade, *Angew. Chem.* **2008**, *120*, 4748; *Angew. Chem. Int. Ed.* **2008**, *47*, 4670.
- [36] B. Siggelkow, M. B. Meder, C. H. Galka, L. H. Gade, *Eur. J. Inorg. Chem.* **2004**, 3424.
- [37] J. Burgess, J. Fawcett, D. R. Russel, S. R. Gilani, *Acta Crystallogr. Sect. C* **2000**, *56*, 649.
- [38] F. A. Cotton, J. S. Wood, *Inorg. Chem.* **1964**, *3*, 245.
- [39] L.-C. Wang, H.-Y. Jang, Y. Roh, V. Lynch, A. J. Schultz, X. Wang, M. J. Krische, *J. Am. Chem. Soc.* **2002**, *124*, 9448.
- [40] G. J. Bullen, *Acta Crystallogr.* **1959**, *12*, 703.
- [41] D. F. Evans, *J. Chem. Soc.* **1959**, 2003.
- [42] D. C. Woska, Z. D. Xie, A. A. Gridnev, S. D. Ittel, M. Fryd, B. B. Wayland, *J. Am. Chem. Soc.* **1996**, *118*, 9102.
- [43] a) R. G. Parr, W. Yang, *Density Functional Theory of Atoms and Molecules*, Oxford University Press, Oxford, **1989**; b) T. Ziegler, *Chem. Rev.* **1991**, 91.
- [44] a) C. Lee, W. Yang, R. G. Parr, *Phys. Rev. B* **1988**, *37*, 785; b) A. D. Becke, *J. Chem. Phys.* **1993**, *98*, 5648; c) P. J. Stephens, F. J. Devlin, C. F. Chabalowski, M. J. Frisch, *J. Phys. Chem.* **1994**, *98*, 11623.
- [45] a) P. J. Toscano, A. L. Seligson, M. T. Curran, A. T. Skrobitt, D. C. Sonnenberger, *Inorg. Chem.* **1989**, *28*, 166; b) R. R. Hung, J. J. Grabowski, *J. Am. Chem. Soc.* **1999**, *121*, 1359; c) G. Li, F. F. Zhang, H. Chem, H. F. Yin, H. L. Chem, S. Y. Zhang, *J. Chem. Soc. Dalton Trans.* **2002**, 105.
- [46] a) A. D. Becke, *Phys. Rev. A* **1988**, *38*, 3098; b) J. P. Perdew, *Phys. Rev. B* **1986**, *33*, 8822.
- [47] a) J. Kuta, S. Patchkovskii, M. Z. Zgierki, P. M. Kozolowski, *J. Comput. Chem.* **2006**, *27*, 1429; b) X.-J. Qi, Z. Li, Y. Fu, Q.-X. Guo, L. Liu, unpublished results.
- [48] a) H. D. Beckey, *Principles of Field Desorption and Field Ionization Mass Spectrometry*, 1st ed., Pergamon, Oxford, **1977**; b) L. Prókai, *Field Desorption Mass Spectrometry*, 1st ed., Marcel Dekker, New York, **1990**.
- [49] a) H. B. Linden, *Eur. Mass Spectrom.* **2004**, *10*, 459; b) H. B. Linden in *Encyclopedia of Mass Spectrometry*, Vol. 8, Elsevier, Amsterdam, **2006**, p. 359.
- [50] a) H. J. Veith, *Mass Spectrom. Rev.* **1983**, *2*, 419; b) J. H. Gross, *J. Am. Soc. Mass Spectrom.* **2007**, *18*, 2254.
- [51] a) F. W. McLafferty, P. F. I. Bente, R. Kornfeld, S.-C. Tsai, I. Howe, *J. Am. Chem. Soc.* **1973**, *95*, 2120; b) K. Levsen, H. Schwarz, *Angew. Chem.* **1976**, *88*, 589; *Angew. Chem. Int. Ed. Engl.* **1976**, *15*, 509.

- [52] D. S. Millington, J. A. Smith, *Org. Mass Spectrom.* **1977**, *12*, 264.
- [53] P. J. Dommelle, R. L. Harlow, S. D. Ittel, W. G. Peet, *Inorg. Chem.* **1983**, *22*, 3944.
- [54] L. W. Deady, O. L. Korytsky, J. E. Rowe, *Aust. J. Chem.* **1982**, *35*, 2025.
- [55] J. H. Gross, N. Nieth, H. B. Linden, U. Blumbach, F. J. Richter, M. E. Tauchert, R. Tompers, P. Hofmann, *Anal. Bioanal. Chem.* **2006**, *386*, 52.
- [56] *SAINT*, Bruker AXS, **2007**.
- [57] R. H. Blessing, *Acta Crystallogr. Sect. A* **1995**, *51*, 33.
- [58] G. M. Sheldrick, *SADABS*, Bruker AXS, **2004–2008**.
- [59] P. T. Beurskens in *Crystallographic Computing 3* (Eds.: G. M. Sheldrick, C. Krüger, R. Goddard), Clarendon, Oxford, **1985**, p. 216; P. T. Beurskens, G. Beurskens, R. de Gelder, J. M. M. Smits, S. Garcia-Granda, R. O. Gould, DIRDIF-2008, Raboud University Nijmegen, The Netherlands, **2008**.
- [60] a) M. C. Burla, R. Caliandro, M. Camalli, B. Carrozzini, G. L. Cascarano, L. De Caro, C. Giacovazzo, G. Polidori, R. Spagna, SIR2004, CNR IC, Bari, Italy, **2004**; b) M. C. Burla, R. Caliandro, M. Camalli, B. Carrozzini, G. L. Cascarano, L. De Caro, C. Giacovazzo, G. Polidori, R. Spagna, *J. Appl. Crystallogr.* **2005**, *38*, 381.
- [61] G. M. Sheldrick, SHELXS-97, University of Göttingen, **1997**.
- [62] G. M. Sheldrick, *Acta Crystallogr. Sect. A* **2008**, *64*, 112.
- [63] G. M. Sheldrick, SHELXL-97, University of Göttingen, **1997**.
- [64] P. van der Sluis, A. L. Spek, *Acta Crystallogr. Sect. A* **1990**, *46*, 194.
- [65] a) A. L. Spek, PLATON, Utrecht University, The Netherlands; b) A. L. Spek, *J. Appl. Crystallogr.* **2003**, *36*, 7.
- [66] Gaussian 03 (Revision D.02), M. J. Frisch, G. W. Trucks, H. B. Schlegel, G. E. Scuseria, M. A. Robb, J. R. Cheeseman, J. A. Montgomery, Jr., T. Vreven, K. N. Kudin, J. C. Burant, J. M. Millam, S. S. Iyengar, J. Tomasi, V. Barone, B. Mennucci, M. Cossi, G. Scalmani, N. Rega, G. A. Petersson, H. Nakatsuji, M. Hada, M. Ehara, K. Toyota, R. Fukuda, J. Hasegawa, M. Ishida, T. Nakajima, Y. Honda, O. Kitao, H. Nakai, M. Klene, X. Li, J. E. Knox, H. P. Hratchian, J. B. Cross, V. Bakken, C. Adamo, J. Jaramillo, R. Gomperts, R. E. Stratmann, O. Yazyev, A. J. Austin, R. Cammi, C. Pomelli, J. W. Ochterski, P. Y. Ayala, K. Morokuma, G. A. Voth, P. Salvador, J. J. Dannenberg, V. G. Zakrzewski, S. Dapprich, A. D. Daniels, M. C. Strain, O. Farkas, D. K. Malick, A. D. Rabuck, K. Raghavachari, J. B. Foresman, J. V. Ortiz, Q. Cui, A. G. Baboul, S. Clifford, J. Cioslowski, B. B. Stefanov, G. Liu, A. Liashenko, P. Piskorz, I. Komaromi, R. L. Martin, D. J. Fox, T. Keith, M. A. Al-Laham, C. Y. Peng, A. Nanayakkara, M. Challacombe, P. M. W. Gill, B. Johnson, W. Chen, M. W. Wong, C. Gonzalez, J. A. Pople, Gaussian, Inc., Wallingford, CT, **2004**.
- [67] a) M. M. Francl, W. J. Pietro, W. J. Hehre, J. S. Binkley, M. S. Gordon, D. J. Defrees, J. A. Pople, *J. Chem. Phys.* **1982**, *77*, 3654; b) W. J. Hehre, R. Ditchfield, J. A. Pople, *J. Chem. Phys.* **1972**, *56*, 2257; c) P. C. Hariharan, J. A. Pople, *Theor. Chim. Acta* **1973**, *28*, 213.

Received: July 7, 2008

Published online: October 22, 2008